Office de la propriété intellectuelle du Canada
Un organisme d'Industrie Canada

Canadian Intellectual Property Office
An Agency of Industry Canada

#3

Bureau canadien des brevets

Certification

Canadian Patent Office

Certification

La présente atteste que les documents ci-joints, dont la liste figure ci-dessous, sont des copies authentiques des documents déposés au Bureau des brevets.

This is to certify that the documents attached hereto and identified below are true copies of the documents on file in the Patent Office.

Specification and Drawings, as originally filed, with Application for Patent Serial No: **2,260,336**, on February 15, 1999, by **HER MAJESTY THE QUEEN IN RIGHT OF CANADA AS REPRESENTED BY THE MINISTER OF INDUSTRY THROUGH THE COMMUNICATION RESEARCH CENTRE AND HER MAJESTY THE QUEEN IN RIGHT OF CANADA AS REPRESENTED BY THE MINISTER OF DEFENCE THROUGH THE DEFENCE RESEARCH ESTABLISHMENT OTTAWA,** for "Modulation Recognition System". The said invention was made while François Patenaude, Martial Dufour, Daniel Bourdreau and Christian Dubuc were employed as a public servants, as defined in the Public Servants Inventions Act in National Defence, pursuant to Section 5 of that Act, the said invention has been determined to be vested in **Her Majesty in right of Canada as represented by the Minister of Industry through the Communication Research Centre and Her Majesty in right of Canada as represented by the Minister of Defence through the Defence Research Establishment Ottawa.**

L. Gregoire

Agent certificateur/Certifying Officer

February 28, 2000

Date

Canada

(CIPO 68)

OPIC CIPO

Field of the Invention

The invention relates to communications signal processing and communication electronics, and particularly to a method for automatic modulation recognition in spectrum monitoring applications.

Background of the Invention

The problem of automating radio frequency spectrum monitoring is of much practical interest. An important aspect of the spectrum monitoring process concerns the classification and identification of individual signals and their sources by evaluating properties of the signals such as the modulation format.

Several methods can be used to tackle the modulation classification problem, as it was shown in C. Dubuc, D. Boudreau, F. Patenaude, "An Overview of Recent Results in AMR", *CRC Technical Memorandum*, VPCS #10/98, March 1998 and R. Lamontagne, "Modulation Recognition: An Overview", *DREO Technical Note*, No. 91-3, March 1991. Some are based on the decision-theoretic approach, which uses probabilistic models to minimize the probability of misclassification errors. These classifiers can achieve very good results at signal-to-noise ratios (SNR) as low as 0 dB. However, they assume knowledge about some of the signal characteristics (e.g. symbol timing). They were also developed for very small digital modulation sets (e.g. BPSK vs. QPSK). Therefore, these techniques appear less suitable for a practical modulation classification system.

Other modulation classification algorithms are based on statistical pattern recognition theory. Automatic modulation recognition approaches based on pattern recognition techniques, such as neural network classification, have recently attracted much attention. A typical idea is to use one or several Artificial Neural Networks (ANN) to process measurements of discriminating features. This type of classifiers shows good results with simulated signals as reported in R. Lamontagne, "An Approach to Automatic Modulation Recognition using Time-Domain Features and Artificial Neural Networks (U)", *DREO Report*, No. 1169, January 1993; S.C. Kremer, "Automatic Modulation Recogntion

Project - Activity Report (Sept. '97- Dec. '98)", Jan. 1998; E.E. Azzouz, A.K. Nandi, *Automatic Modulation Recogntion of Communications Signals*, Klewer Academic Press, Boston, 1996, 217 p.; A.K. Nandi, E.E. Assouz, "Algorithms for Automatic Modulation Recognition of Communication Signals", *IEEE Trans. on Comm.*, Vol. 46, No. 4, April 1998, pp. 431-436; and E.E. Azzouz, A.K. Nandi, "Automoatic Modulation Recogntion - I & II", *J. Franklin Inst.*, Vol. 334B, No. 2, pp. 241-305, 1997. However, the performance of neural networks in a practical system is highly dependent upon the training set. Since neural networks can perform "learning vector quantization", they can achieve an efficient class definition over a large multi-dimensional feature space. The key issue is to identify a set of meaningful features, and to train the network properly. One problem is that the network can become so sharp at recognizing the training vectors that it performs erroneously when presented with on-line data that differs only slightly from that of the training set. Furthermore, the algorithm designer loses much control on the classification algorithm, and has more difficulty in applying *a priori* knowledge of the taxonomy of modulation types.

Another pattern recognition technique used for automatic modulation recognition is the decision tree algorithm. Results from Azzouz and Nandi as reported in E.E. Azzouz, A.K. Nandi, *Automatic Modulation Recogntion of Communications Signals*, Klewer Academic Press, Boston, 1996, 217 p.; A.K. Nandi, E.E. Assouz, "Algorithms for Automatic Modulation Recognition of Communication Signals", *IEEE Trans. on Comm.*, Vol. 46, No. 4, April 1998, pp. 431-436; and E.E. Azzouz, A.K. Nandi, "Automoatic Modulation Recogntion - I & II", *J. Franklin Inst.*, Vol. 334B, No. 2, pp. 241-305, 1997, show that a decision tree can achieve a performance comparable to an ANN classifier when using the same features. A comparison of their ANN and decision tree classifiers is shown in Table 1.

SNR (dB)	Decision Tree	ANN
5	61.3%	60.9%
10	87.9%	88.1%
15	94.6%	96.3%
20	94.6%	96.4%

Table 1 - Overall success rate comparison between the ANN and the decision tree classifiers of Azzouz and Nandi for an ensemble of modulation types.

Furthermore, a decision tree involves a much lower computational complexity than that of a neural network. This is mainly due to the highly hierarchical structure of the tree. Only a subset of features is calculated in order to classify a signal, instead of all the set for a neural network. Knowing that in both cases, the largest amount of computations come from the features, there is an obvious computational gain coming from the use of a hierarchical structure. However, the known pattern recognition techniques using a decision tree algorithm do not achieve good performance at signal-to-noise rations (SNRs) below 0 dB.

Summary of the Invention

It is now an object of the invention to provide a more straightforward and computationally simpler method of modulation recognition than neural network based methods.

It is another object of the invention to provide a modulation recognition method which directly exploits the fundamental characteristics of the potential signals to evaluate a decision tree.

It is a further object of the present invention to provide a modulation recognition method with a range of successful classification which is extended to lower signal-to-noise ratios (SNR), preferably as low as 5 dB.

It is yet another object of the invention to provide a modulation recognition method for identification of the following modulation set:

Continuous Wave (CW), Amplitude Modulation (AM), Double Sideband Suppressed Carrier (DSB-SC), Frequency Modulation (FM), Frequency Shift Keying (FSK), Binary Phase Shift Keying (BPSK), Quaternary Phase Shift Keying (QPSK) modulations and MPSK/QAM/OTHER

It is still a further object of the invention to provide a modulation recognition method wherein the requirements for *a priori* knowledge of the signals are minimized by the inclusion of a carrier frequency construction step. Accordingly, the invention provides a method for estimating the noise floor of a signal, comprising the steps of

examining the signal for amplitude variations for identifying the signal as one of an envelope and non-constant envelope signal;

estimating the carrier frequency and correcting for carrier frequency errors; and

categorizing the modulation of the signal.

When the signal is identified as a constant envelope signal, the step of estimating the carrier frequency preferably includes the steps of processing the signal by a Test Fourier Transform (TFT) of the input signal, determining the square of the absolute value obtained, and searching for the maximum frequency sample.

In a preferred embodiment, the TFT is with zero padding. Furthermore, the step of searching preferably includes a coarse search and a fine search.

When the signal is identified as a non-constant envelope signal, the step of estimating the carrier frequency includes the steps of

in a first path, processing the signal by a Fast Fourier Transform (FFT) to produce a first output;

in a second path, passing the signal through a square law non-linearity before processing by a FFT to produce a second output;

in a third path, passing the signal through a fourth law non-linearity before processing by a FFT to produce a third output; and

selecting a maximum energy sample among the first, second and third outputs as a normalized frequency estimate;

whereby the first path is selected when the signal is an AM signal, the second path is selected when the signal is a DSB-SC or BPSK signal, and the third path is selected when the signal is a QPSK signal.

Brief Description of the Drawings

A preferred embodiment of the invention will be further described in more detail with reference to the attached drawings, wherein:

FIG. 1 is a functional flow chart of the decision tree of the preferred embodiment of the method in accordance with the invention.

FIG. 2 shows the squared Discrete Fourier Transform (DFT) coefficients of a QPSK signal at a SNR of 5dB;

FIG. 3 shows the squared DFT coefficients of a FM signal at a SNR of 5 dB;

FIG. 4 shows an instantaneous frequency histogram for a binary FSK signal at a SNR of 5 dB;

FIG. 5 illustrates the phase processing for instantaneous frequency calculation;

FIG. 6 shows a phase processed instantaneous frequency histogram for a FSK signal at a SNR of 5 dB;

FIG. 7 shows a DSB-SC signal;

FIG. 8 shows a DSB-SC signal with absolute values;

FIGS. 9 and 10 show typical power spectrums for real and pseudo voice signals respectively;

FIG. 11 shows a comparison between the recognition success rates achievable with prior art methods and that of the present method;

FIG. 12 is an overall success rate comparison with a prior art method;

FIG. 13 is a performance comparison between a DREO classifier and a classifier of the present invention.

FIG. 14 is a graph illustrating the success rate of the modulation recognition method of the invention against the frequency offset for SNR=15dB;

FIG. 15 is a graph illustrating the success rate of the modulation recognition method of the invention against the frequency offset for SNR=5dB;

FIG. 16 is a flow chart of the frequency construction methof for constant envelope signals; and

FIG.17 is a flow chart of the frequency estimation method for non-constant envelope signals.

Detailed Description of the Preferred Embodiment

The first fundamental characteristic that the classifier method in accordance with the invention examines is the presence of significant amplitude variations in the observed signal received over an Additive White Gaussian Noise (AWGN) channel. This first binary test allows an initial discrimination between frequency (analog or digital) modulated and amplitude or phase (analog or digital) modulated signals. Since this test is also insensitive to frequency errors (within the observed bandwidth constraint), it allows a subsequent carrier frequency estimation that takes advantage of the absence or presence of amplitude variations. This point is very important, since most of the published work about automatic modulation recognition assumes a perfect knowledge of the carrier frequency, and does not disclose any methods to acquire this knowledge.

More detailed information is obtained by applying additional binary tests as described further below for estimation of the carrier frequency error. The results of simulations presented in Example I below show the good characteristics of the estimation method, for the modulation formats in the set {CW, AM, DSB-SC, FM, FSK, BPSK, QPSK, *M*PSK-QAM}.

A flowchart of the preferred decision tree in accordance with the present invention is shown in Fig. 1. It is briefly described in the following paragraph. Its specific components are discussed in detail further below.

The first step of the preferred modulation categorization method determines if there are significant amplitude variations in the observed signal. The class of signals with little amplitude fluctuations (constant envelope) is easily decomposed, after correction for carrier frequency errors, into the classes of unmodulated signals (CW) and FM modulated signals. This last class is further split in another step into analog FM and digital FM (FSK). The class of amplitude modulated signals (non-constant envelope), after being corrected for carrier frequency errors, is readily divided in a further step between the one-dimensional (AM, DSB-SC, BPSK) and the two-dimensional (QAM, PSK) signals. The fundamental phase characteristics of the one-dimensional signals allow the recognition of the AM signals, from the two other formats. The DSB-SC signal vectors having more amplitude variations than BPSK signals, they can be identified with a simple test. The remaining signals are classified as BPSK signals, although the QPSK signals with constellation points that are members of the set $[\pi/4, 3\pi/4, 5\pi/4, 7\pi/4]$ can also be recognized at this stage.

The next few sections present the different tests used in the decision tree. Each test consists in a comparison of a feature extracted from the received signal segment with a fixed threshold. The result of this test determines the next branch to be used.

Constant vs non constant envelope signals

The first step in the preferred modulation recognition method of the invention is to identify the constant envelope signals (CW, FM, FSK). PSK signals are not considered as constant envelope signals, since practical PSK signals are band-limited, therefore having a non constant envelope.

The feature used to identify the envelope variations has been introduced in A.K. Nandi, E.E. Azzouz, "Automatic Analog Modulation Recognition", *Signal Processing*, V. 46, 1995, pp. 211-222 and is the maximum of the Squared Fourier Transform of the normalized signal amplitude. It is defined as

$$\gamma_{max} = \max_{f} \frac{|DFT(\underline{a}_{cn})|^2}{N_s} \qquad (1)$$

where f is the frequency, DFT( ) is the Discrete Fourier Transform, N_s is the number of samples in the sequence and $\underline{a}_{cn}$ is the amplitude vector centered on zero and normalized by its mean. Mathematically, $\underline{a}_{cn}$ is expressed as

$$\underline{a}_{cn} = \frac{|\underline{x}|}{E[|\underline{x}|]} - 1 \qquad (2)$$

where $\underline{x}$ is the received signal vector.

This feature is a measure of the information in the envelope and allows the separation of constant envelope formats from non constant envelope signals, even PSK signals. In fact, PSK signals have a periodical fluctuation in the envelope, corresponding to the symbol transitions. These fluctuations will cause high energy coefficients, at the symbol rate, in the DFT of the centered normalized envelope.

The squared DFT coefficients for a QPSK signal at a SNR of 5 dB are shown in Figure 2. Note that the highest values correspond to the symbol rate (4 kbauds, in this case). This information can therefore be used as an estimate for the symbol rate of the PSK and QAM signals. The squared DFT coefficients for a FM signal, also at a SNR of 5 dB, are shown in Figure 3.

For the FM signal, all the coefficients are approximately the same and have a small value. Even if the SNR is small, the maximum value of these normalized coefficients can be used

as an efficient feature to recognize constant envelope signals. It gives better results than simply using the variance of the normalized envelope, because is it less sensitive to noise. Amplitude modulated signals with low modulation indexes are also characterized with this method.

Frequency Estimation and Correction

A key point in the proper operation of the decision tree of Fig. 1 is the reliable estimation of frequency errors. As indicated in the above, the first test on the presence of amplitude variations is insensitive to carrier frequency errors, which allows the subsequent selection of frequency estimation steps that take advantage of the information obtained through this first test.

There are then two different carrier frequency estimation steps. If the observed signal is classified as constant-envelope, then it is assumed that this signal is unmodulated (CW). The estimation method of Fig. 16 is then applied. It involves the identification of the maximum energy frequency sample in the frequency domain representation of the signal, which, in the case of a baseband CW signal, corresponds to the estimate of the frequency offset as reported in A.K. Nandi, E.E. Azzouz, "Algorithms for Automatic Modulation Recognition of Communication Signals", *IEEE Trans. on Comm.* Vol. 46, No. 4, April 1998, pp. 431-436. If the hypothesis that the signal is unmodulated is true, the proper frequency offset is obtained. If the hypothesis is false, the frequency estimate is much less precise, but the test on the unwrapped phase produces a decision in favor of the FM-FSK signals even if a residual frequency error still exists. The estimation method includes the steps of processing the input signal by a fast Fourier transform (FFT) of the input signal, obtaining the square of the absolute value obtained and searching for the maximum frequency sample. The FFT is preferably with zero padding. The step of searching preferably includes a coarse search and a fine search.

If the observed signal bears significant envelope fluctuations, the frequency estimation method is that of Fig. 17. In this case, the implicit assumption is that the signals are not two-dimensional, except for QPSK. The observed signal flows in three paths, where its samples are either processed directly by an FFT, or passed through a square law or a fourth law

nonlinearity, before the FFT. The frequency corresponding to the maximum energy sample among the outputs of the three paths is taken as the normalized frequency estimate. If the signal is AM, the $M = 1$ path is selected, if it is DSB-SC or BPSK, the $M = 2$ path is selected, and if it is QPSK, the $M = 4$ path is retained. If any other form of signal is observed, the frequency estimate will be erroneous, which results in a signal with a large phase variance, and in a correct classification as a two-dimensional signal.

Frequency Modulated Signals vs CW

Once frequency correction has been performed, CW signals are distinguished from frequency modulated signals by examining the time history of the instantaneous phase. Assuming a perfect correction of the carrier frequency, a CW signal has a constant phase. The variance of the unwrapped phase is a good feature representing the variability of the phase. CW signals have a near-zero variance of the unwrapped phase, while frequency modulated signals have a high variance. However, the instantaneous phase of a sampled signal is very sensitive to noise if the amplitude is small. The variance due to noise on the instantaneous phase of a sample will vary with its amplitude. Weak samples will have a higher variance on their phase than strong samples, since the phase variations increase as the SNR decreases. To avoid this problem, a threshold is set on the amplitude of the signal. The problem can be minimized by discarding any phase data for which the corresponding amplitude is below the threshold. The higher the threshold is set, the lower the residual phase variance is for a CW signal, without affecting the phase variance of frequency modulated signals. A threshold equal to the mean of the amplitude of the signal is chosen. A higher threshold increases the possibility of discarding an entire noise-free constant envelope signal. The distinction between CW and frequency modulated signals is therefore obtained by comparing the value of the variance of the unwrapped phase (direct phase) to a phase threshold, for the samples bearing an amplitude above their mean. The appropriate phase threshold can be obtained by using computer simulations as described further below.

Digital vs Analog Frequency Modulation (FSK vs FM)

The instantaneous frequency distribution can be used to identify the modulation type for frequency modulated signals. Using directly the instantaneous frequency histogram as a set of features is known in the art as reported in E.E. Azzouz, A.K. Nandi, *Automatic Modulation Recognition of Communications Signals*, Klewer Academic Press, Boston, 1996, 217p.5. However, it is possible to characterize a distribution by its mean, variance, skewness and kurtosis coefficients in order to reduce the number of features. Among these parameters, the kurtosis coefficient produces good results as reported in[R. Lamontagne, "An Approach to Automatic Modulation Recognition using Time-Domain Features and Artificial Neural Networks (U)", *DREO Report*, No. 1169, January 1993. This coefficient is defined as the fourth normalized moment, centered about the mean, of the instantaneous frequency, defined as

$$\mu_{42}^{f} = \frac{E[f_i^4(t)]}{\left(E[f_i^2(t)]\right)^2}, \qquad (3)$$

where $f_i(t)$ is the instantaneous frequency (about the mean) at time t. The kurtosis coefficient is a measure of the flatness of the distributions. Since this is usually different for analog and digitally frequency modulated signals, it can be used as a feature for distinguishing between FSK and FM signals.

The instantaneous frequency is obtained by computing the phase derivative of the observed signal. However, the calculation of instantaneous frequency is very sensitive to noise, since the instantaneous frequency is the derivative of the instantaneous phase. The derivative operator has a linear gain increasing with the frequency. Therefore, it amplifies higher frequency noise, especially the one not in the band of interest, and attenuates the useful signal. The instantaneous frequency histogram for a binary FSK signal at a SNR of 5 dB is shown in Figure 4. In this case, the instantaneous frequency distribution of a FM signalis difficult to recognize. This is reflected in the kurtosis coefficient calculation, which has a large value.

Since it is known at this point that the signal is frequency modulated, a simple way to decrease the effect of higher frequency noise enhancement is to filter the phase signal before passing it through the derivative. The phase signal has about the same bandwidth as the modulating signal. A simple algorithm roughly estimates the effective bandwidth of the phase signal and picks a low-pass filter in a library, with a cutoff frequency slightly higher than the signal bandwidth. A very small library of filters can be used. Figure 5 shows the phase processing needed before taking the derivative of the phase signal.

Using this pre-filtering technique, the resulting noise in the instantaneous frequency sequence is much less important. As an example, using the same signal as the one used to obtain Figure 4, the proposed phase processing is applied with a filter having a cutoff frequency 1.5 times larger than the useful phase signal bandwidth. The resulting instantaneous frequency histogram is shown in Figure 6. Even for human eyes, it is clear that the distribution of this instantaneous frequency signal is easier to recognize from that of an FM signal. Two peaks can easily be identified, giving even an idea of the frequency deviation.

In this case the kurtosis coefficient of the instantaneous frequency is very low (approximately 1.36). It is 2.83 without the phase filtering. FM signals usually have a kurtosis coefficient above 2.5. Thus, there is a significant performance gain achievable by filtering the phase signal before the derivation.

Because the decision based on the coefficient of kurtosis is largely insensitive to frequency offsets, the discrimination between FM and FSK signals is performed directly on the observed signal. This allows a simplification in the frequency estimation.

One-Dimensional Signals (AM, DSB-SC, BPSK) vs Two-Dimensional Signals

For the non-constant envelope signals, the second step of the preferred method in accordance with the invention is to identify signals which have no information in their phase. In the absence of frequency or phase errors, these signals correspond to real baseband signals, such

as AM (transmitted carrier), DSB-SC and BPSK signals. These signals can be recognized from their absolute centered unwrapped phase sequence, as proposed in R. Lamontagne, "An Approach to Automatic Modulation Recognition using Time-Domain Features and Artificial Neural Networks (U)", *DREO Report*, No. 1169, January 1993. Although the absolute phase of the real baseband signals normally has a small variance, phase unwrapping is necessary in practice because the initial carrier phase is random. However, phase unwrapping is very sensitive to noise, particularly for DSB-SC and BPSK signals, due to their 180° phase transitions. Consequently, phase unwrapping is undesirable since any phase unwrapping errors will seriously increase the variance of the absolute centered phase.

To avoid phase unwrapping of DSB-SC and BPSK signals, a new quantity is used as the method in accordance with the invention, the "absolute" phase, which is defined as

$$\phi_a(t) = \angle\left(|I(t)| + j|Q(t)|\right), \qquad (4)$$

where $I(t)$ and $Q(t)$ are the inphase and quadrature samples at time t. Taking the absolute values of the real and imaginary parts of a signal yields a phase sequence between 0 and $\pi/2$ radians, which allows a significant reduction in the size of the observation space required to produce a decision. Figure 7 shows the original DSB-SC signal and Figure 8 shows the resulting signal when the absolute value of the real and imaginary parts are taken.

It can be seen that, for a DSB-SC signal, the variance of the phase of the resulting signal is small. This is also true for BPSK and AM signals. For two-dimensional signals bearing some phase information, the variance of the absolute phase is high, tending toward the variance of a uniformly distributed random variable in the interval $[0, \pi/2]$ radians. To allow a better separation of one and two-dimensional baseband signals, a threshold on the amplitude of the signal is also used (i.e. the samples below this threshold are discarded). This procedure reduces the variance of the phase for one-dimensional signals, without affecting significantly the variance for two-dimensional signals. The best results occur when the threshold is set equal to the mean of the amplitude of the sequence, as can be seen from simulation as described further below.

AM vs DSB-SC/BPSK Signals

BPSK signals can be viewed as DSB-SC signals modulated by a binary Non-Return-to-Zero (NRZ) sequence. These signals, unlike AM signals, have jumps of radians in their instantaneous phase sequence. The simplest way to distinguish them from AM signals, is to directly look at the variance of the unwrapped phase (direct phase). AM signals have a lower phase variance than DSB-SC and BPSK, due to the frequent phase jumps of radians. As explained before, phase unwrapping is difficult for DSB-SC and BPSK signals. However, since the expected variance in the phase is high for these signals, phase unwrapping errors are relatively unimportant. Furthermore, AM signals are not likely to produce phase unwrapping errors. In this preferred method, a threshold (equal to the mean amplitude) is set on the amplitude of the samples, in order to reduce the phase variance for AM signals. ASK modulation is a digital form of amplitude modulation (AM). ASK signals are therefore classified as AM signals. Further processing would be required to recognize them from analog AM signals.

DSB-SC vs BPSK

Unlike BPSK signals, DSB-SC signals have envelopes whose amplitudes vary substantially over time. Consequently, the variance of the envelope can be used as a feature for recognizing BPSK signals from DSB-SC signals. However QPSK signals that have been previously classified as real baseband signals will be classified as BPSK signal, since they also have an almost constant envelope.

Binary vs Quarternary PSK Signals

A side effect of using the absolute phase feature for discriminating between one-dimensional and two-dimensional signals, is that some QPSK signals can be classified as one-dimensional baseband signals. This happens when the transmitted symbols correspond to the constellation points in the set $\{\pi/4, 3\pi/4, 5\pi/4, 7\pi/4\}$ radians. In this case, taking the absolute value of the real and imaginary parts brings all the symbols to $\pi/4$ radians. These signals then mimic the

behavior of BPSK signals. One method to differentiate between the binary and the quaternary cases is to rotate the signal by $\pi/4$ radians. If the signal is QPSK, its constellation points then correspond to the angles $\{ \pi/2, , 3\pi/2\}$ radians. Once this rotation is done, the test on the absolute phase is repeated. For BPSK signals, the results do not change significantly. For QPSK signals, the variance on the "absolute" phase is very high, since the symbols then often jump between 0 and $\pi/2$ radians.

The Class of Two-Dimensional Signals

The class of two-dimensional signals is not further processed in the present method.

Example I

Simulations

To characterize the methods of Figs 1 to 3, 500 simulated signals of each of the modulation types have been generated and processed in the Matlab environment. These 500 signals cover a range of parameters (e.g. modulation index, symbol rate, pulse shaping filters), as detailed in the next paragraphs. A sampling frequency of 48 kHz is used, covering a bandwidth slightly larger than the occupied bandwidth of most narrowband communications signals

Sequences of 100 ms (4800 samples) were used as inputs to the classifier. Complex baseband signals were used, and carrier frequency and phase errors were simulated. The frequency error is random and uniformly distributed over the range [–4.8 kHz, 4.8 kHz], while the initial carrier phase is uniformly distributed over $[-\pi, \pi]$. For digitally modulated signals, a random delay, uniformly distributed over $[0, T_s]$ (where T_s is the sampling period), was applied to simulate symbol timing uncertainties.

The Simulation of Specific Signals

For analog modulation schemes, two types of source signals were simulated. First, a real voice signal, band-limited to [0, 4 kHz], was used. The second source signal was a simulated voice signal using a first order autoregressive process of the form

$$y[k] = 0.95 \cdot y[k-1] + n[k], \tag{5}$$

where $n[k]$ is a white Gaussian noise process. This pseudo-voice signal was further bandlimited to [300, 4000 Hz]. The use of a first order autoregressive process to simulate voice was proposed in[S.C. Kremer, "Automatic Modulation Recognition Project - Activity Report (Sept. '97 - Dec. '98)", Jan. 1998. Typical power spectrums are shown for real and pseudo voice signals, on Figure 9 and Figure 10 respectively. The major difference between the real and the pseudo voice signals is the presence of pauses in the real signal. In the pseudo voice signal, the signal is present 100% of the time. This leads to different results, since unmodulated (or slightly modulated) 100 ms-long sequences can be observed with the real voice signal.

For AM signals, a constant value was added to the source signal. The modulation index was uniformly distributed in the interval [50%, 100%]. The modulation index was calculated using the maximum amplitude value over the whole source signal. The total length of the source signal was about 120 seconds for the real signal, and 40 seconds for the pseudo-voice sequence. From these source signals, 100 ms-long sequences were extracted randomly. Therefore, the observed modulation index for a sequence was less or equal to the chosen modulation index.

For frequency modulated signals, a cumulative sum was used to approximate the integral of the source signal. Generic FM signals were simulated using real or pseudo-voice signals,

with a modulation index uniformly distributed in the interval [1, 4]. The bandwidth occupied by these signals was therefore between 16 kHz and 40 kHz, using the approximation

$$BW \approx 2(\beta + 1) f_{max}, \qquad (6)$$

where β is the modulation index and f_{max} is the maximum source frequency (4 kHz in this case). The analog Advanced Mobile Phone Service (AMPS) FM signals were approximated using a modulation index of 3.

Continuous-phase FSK signals were simulated by using filtered *M*-ary symbols to frequency modulate a carrier. Pager signal parameters were based on observations of real signals, with 2FSK modulation a bit rate of 2400 bps, a frequency deviation of 4.8 kHz and almost no filtering. 4FSK signals were also simulated, using the same frequency deviation and a symbol rate of 1200 baud. The 19.2 kbps 2FSK signals from the Racal Jaguar Radio were simulated using a frequency deviation of 6.5 kHz and a 5th order Butterworth pre-modulation filter, with a cutoff frequency of 9.6 kHz.

For PSK and QAM signals, symbols were filtered with either a raised cosine or a square-root raised cosine function. The selection was randomly performed with equal probabilities. The rolloff factors of 20, 25, 30, 35, 40, 45 and 50% were uniformly and randomly selected. For all these signals, the symbol rates were chosen randomly between 4, 5, 8, 10, 16 and 20 kbaud. π/4-QPSK signals similar to IS-54 signals were also simulated, with a symbol rate of 24 kbaud and a square-root raised cosine pulse shaping filter with a rolloff factor of 35%.

Additive Noise

The simulated signals were passed through an additive white Gaussian noise channel before being classified. Note that no filtering was done at the receiver, so the signal observed by the classifier was corrupted by white noise. The noise power was calculated from the knowledge of the average power of the modulated signal and of the SNR over the sampling bandwidth. This SNR was defined as

$$\mathrm{SNR}_{samp} = \frac{S}{N_0 \cdot F_s}, \qquad (7)$$

where S is the signal power, N_0 is the white noise power spectral density and F_s is the sampling frequency equal to 48 kHz.

For amplitude modulated signals (AM, DSB-SC and SSB), the average power was calculated using the whole source signals (real and pseudo-voice). This implies that, for a given sequence, the observed SNR might be different from the global SNR. This is especially true for DSB-SC and SSB signals, where some segments of the signals may have no power at all.

Table 2 shows the mean observes SNR for the 200 simulated signals of each modulation types and the standard deviation ( ) when the desired SNR is 15 dB. Note the results for DSB-SC signals using real voice.

Modulation Schemes	Mean SNR_{samp} (dB)	σ (dB)
CW	15.0049	0.0671
AM (V)	15.0107	0.0834
AM (PV)	15.0035	0.0526
DSB-SC (V)	4.6926	14.5438
DSB-SC (PV)	14.9865	0.3982
SSB (V)	6.0157	13.9455
FM (V)	14.9999	0.0619
FM (PV)	14.9932	0.0633
FM (AMPS) (V)	15.0011	0.0644
FSK (Pager)	14.9711	0.0671
FSK4	14.9936	0.0689
FSK (Jaguar)	14.9367	0.0673
BPSK	14.9931	0.0664
QPSK	14.9910	0.0615
PSK8	14.9843	0.0678
π/4-QPSK (IS-54)	14.9863	0.0641
QAM16	14.9868	0.1143
V: Voice PV: Pseudo Voice		

Table 2 - Observed SNRs (15dB).

Example II

Binary Decision Thresholds

In the disclosed decision tree, each decision consists in a comparison of a signal feature with a threshold. For the simulations, these thresholds have been set using the results of direct observations of the feature distributions in a training set of simulated signals having a SNR of 5 dB. More optimal thresholds can be obtained using empirical results for real signals. The selected thresholds are summarized in Table 3 for the different features.

Feature	Threshold
Maximum of the normalized squared FFT of the centered normalized envelope (γ_{max})	1.44
Variance of the unwrapped phase (rad) (CW vs. FM/FSK)	0.16
Variance of the unwrapped phase (rad) (AM vs. DSB-SC/BPSK)	4.0
Variance of the "absolute" phase (rad)	0.144
Kurtosis of the instantaneous frequency	2.5
Variance of the normalized amplitude	0.25

Table 3: Decision thresholds used in the simulations.

Example III

Phase Filter Selection for FM/FSK Separation

As discussed above, lowpass filters are required to eliminate the increased high frequency noise resulting when the derivative of the phase is obtained. 10^{th} order lowpass Butterworth filters were used in the simulations. For each modulation type, a bandwidth larger than the maximum bandwidth of the phase signal was selected. In Table 4, the selected cutoff frequencies for the lowpass filters are presented. Note that these cutoff frequencies are not very tight with respect to the maximum frequency content of the phase signal.

Modulation schemes	Cutoff frequency
All analog FM signals	9.6 kHz
Pager signals (2FSK)	7.2 kHz
Jaguar radio signals (2FSK)	12 kHz
4FSK	12 kHz

Table 4: Phase filter cutoff frequencies.

Example IV

Classification Results

An estimate of the performance of the modulation classification method of the invention was obtained by using the previously described simulated signals. For each modulation type, the 500 generated sequences were classified using the preferred method of Fig. 1. There are 8 possible outputs from the classification system: CW, AM, DSB-SC, FM, FSK, BPSK, QPSK, *M*PSK/QAM/OTHER ($M > 2$). Tables 5 to 8 show the classification results for each of the simulated modulation types at SNRs of 5 and 10 dB. Tables 5 and 7 indicate the classification accuracy when the frequency errors are zero, while Tables 6 and 8 present the performance when the frequency error is a random variable, uniformly distributed between −4.8 kHz and 4.8 kHz (i.e. ± 10% of the sampling frequency). Comparing these two sets of

tables indicates that the frequency estimation and correction steps of the present method perform very well, and degrade the overall performance only slightly.

Modulation	CW	AM	DSB-SC	FM	FSK	BPSK	QPSK	MPSK QAM OTHER
CW	98%	2%						
AM (V)	55.8%	43.8%				0.2%		0.2%
AM (PV)	12%	88%						
DSB-SC (V)			43.6%					56.4%
DSB-SC (PV)			100%					
FM (V)	3.2%	0.2%		93.4%	1%			2.2%
FM (PV)				98.6%				1.4%
FM (AMPS) (V)		0.2%		96%	2.8%			1%
FSK (pager)					97.2%			2.8%
FSK (Jaguar)				1.6%	94.2%			4.2%
4FSK					98.6%			1.4%
BPSK						100%		
QPSK				0.4%	0.4%		7.2%	94.5%
/4-QPSK (IS-54)				3.8%	4.2%			92%
8PSK					1.2%			98.8%
16QAM								100%
SSB (V)								100%

Table 5: Classification results for no error in the carrier frequency at SNR = 5 dB.

Modulation	Classified as							
	CW	AM	DSB-SC	FM	FSK	BPSK	QPSK	MPSK QAM OTHER
CW	98%	2%						
AM (V)	55.8%	43.8%		0.2%		0.2%		
AM (PV)	12%	88%						
DSB-SC (V)			42.2%					57.8%
DSB-SC (PV)			100%					
FM (V)	2.6%	0.4%		94%	1%			2%
FM (PV)				98.6%				1.4%
FM (AMPS) (V)		0.2%		96.2%	2.6%			1%
FSK (pager)					97.2%			2.8%
FSK (Jaguar)				6.6%	89.2%			4.2%
4FSK					98.6%			1.4%
BPSK						100%		
QPSK				0.2%	0.6%		7.4%	91.8%
/4-QPSK (IS-54)				4.6%	3.4%		1%	92%
8PSK				0.2%	1%			98.8%
16QAM								100%
SSB (V)		2%	0.6%				1.2%	96.2%

Table 6: Classification results for random errors in the carrier frequency at SNR = 5 dB.

Modulations	Classified as:							
	CW	AM	DSB-SC	FM	FSK	BPSK	QPSK	*M*PSK QAM OTHER
CW	100%							
AM (V)	58.2%	41.8%						
AM (PV)	11.6%	88.4%						
DSB-SC (V)			61%					39%
DSB-SC (PV)			100%					
FM (V)	12%			84.6%	3.4%			
FM (PV)				100%				
FM (AMPS) (V)	4.8%			90.8%	4.4%			
FSK (pager)					100%			
FSK (Jaguar)				1.2%	98.8%			
4FSK					100%			
BPSK						100%		
QPSK							34.2%	65.8%
/4-QPSK (IS-54)				3.6%	5%			91.4%
8PSK								100%
16QAM								100%
SSB (V)								100%

Table 7: Classification results for no error in the carrier frequency at SNR = 10 dB.

	Classified as							
Modulation	CW	AM	DSB-SC	FM	FSK	BPSK	QPSK	*M*PSK QAM OTHER
CW	100%							
AM (V)	58.2%	41.8%						
AM (PV)	11.6%	88.4%						
DSB-SC (V)			59.8%					40.2%
DSB-SC (PV)			100%					
FM (V)	12.6%			84.6%	2.8%			
FM (PV)				100%				
FM (AMPS) (V)	6.2%			89.6%	4.2%			
FSK (pager)					100%			
FSK (Jaguar)				4%	96%			
4FSK					100%			
BPSK						100%		
QPSK							33.6%	66.4%
/4-QPSK (IS-54)				2.4%	6.2%		27%	64.4%
8PSK								100%
16QAM								100%
SSB (V)		4.8%	2.6%			0.2%	0.6%	91.8%

Table 8 : Classification results for random errors in the carrier frequency at SNR = 10 dB.

A very important result obtained from these simulations is the fact that the classification method in accordance with the invention performs well for SNRs as low as 5 dB. Prior-art simulations have shown that an abrupt performance degradation occurs between 0 dB and 5 dB. This good performance is related to the fact that the binary decision thresholds used in the present classifier were determined at a SNR of 5 dB. This performance is as good or better than most algorithms based on pattern recognition techniques (neural networks), which usually have threshold SNRs on the order of 10 to 15 dB as discussed in R. Lamontagne, "An Approach to Automatic Modulation Recognition using Time-Domain Features and Artificial Neural Netwoks (U)", *DREO Report*, No. 1169, January 1993.

In examining the tables, it is important to remember that QPSK signals can be classified either as QPSK or *M*PSK/QAM/OTHER ($M > 2$) signals. Therefore, the probability of classifying a QPSK signal in either of these categories is 100%. One of the most important results to extract from these tables is the difference between the classification of analog modulation signals using real or simulated voice. For these modulations, the pauses in a real voice source produce unmodulated sequences. For DSB-SC and SSB signals, these pauses produce no signal at all. If the 100 ms preferably used by the present classification method is mostly a pause, the signal is classified as noise, i.e. *M*PSK/QAM/OTHER signal. For AM and FM signals, the absence of a source signal produces a CW. Therefore, quiet sequences are classified as CW signals in these cases. This result can be easily measured by comparing analog modulated signals using real or pseudo-voice sources. Pseudo-voice signals are used to measure the performance of the classification method when the signal is modulated. Real voice signals are used to measure the expected performance of the system in a real environment.

Dynamic thresholds could be used in the different tests of the decision tree to improve the performance of the classification method. If a good estimate of the SNR is available, it

could be used to modify some thresholds. This would be particularly useful in the recognition of AM signals from CW signals. If an estimate of the *a priori* probabilities is also available, thresholds could be modified to minimize the probability of error.

The modular nature of the estimation algorithm simplifies its extension to additional modulation types. Also, although the disclosed approach implicitly assumes an AWGN channel, there are possibilities of extending it to more complex channel models by employing additional processing such as blind equalization.

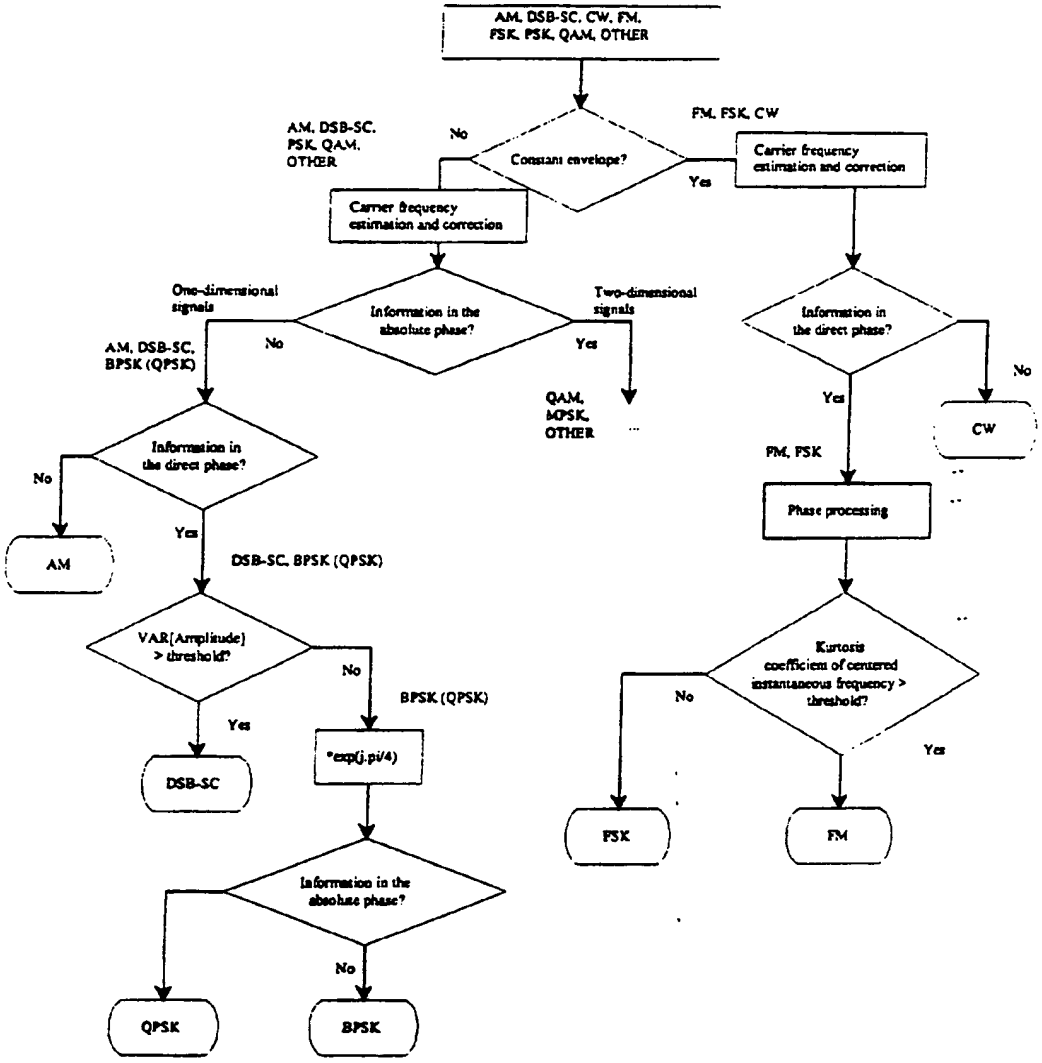
AM, DSB-SC, CW, FM, FSK, PSK, QAM, OTHER
AM, DSB-SC, PSK, QAM, OTHER
No
Constant envelope?
FM, FSK, CW
Yes
Carrier frequency estimation and correction
Carrier frequency estimation and correction
One-dimensional signals
Information in the absolute phase?
Two-dimensional signals
No
Yes
AM, DSB-SC, BPSK (QPSK)
QAM, MPSK, OTHER
Information in the direct phase?
No
Yes
AM
DSB-SC, BPSK (QPSK)
VAR(Amplitude) > threshold?
No
Yes
BPSK (QPSK)
DSB-SC
*exp(j.pi/4)
Information in the absolute phase?
No
QPSK
BPSK
Information in the direct phase?
Yes
No
CW
FM, FSK
Phase processing
Kurtosis coefficient of centered instantaneous frequency > threshold?
No
Yes
FSK
FM

Figure 1

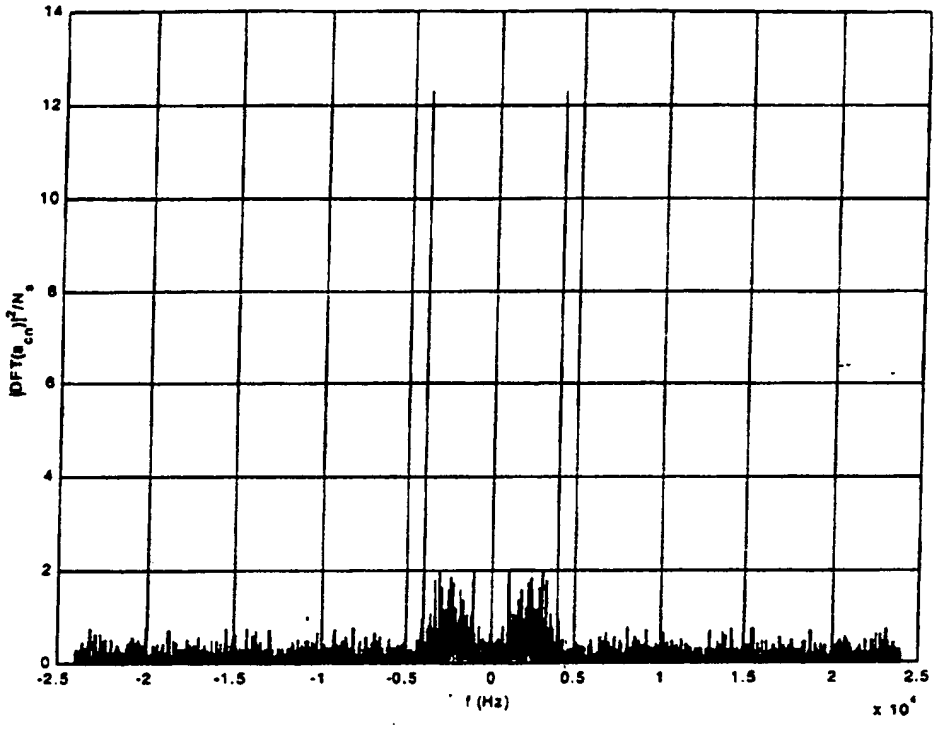

Figure 2

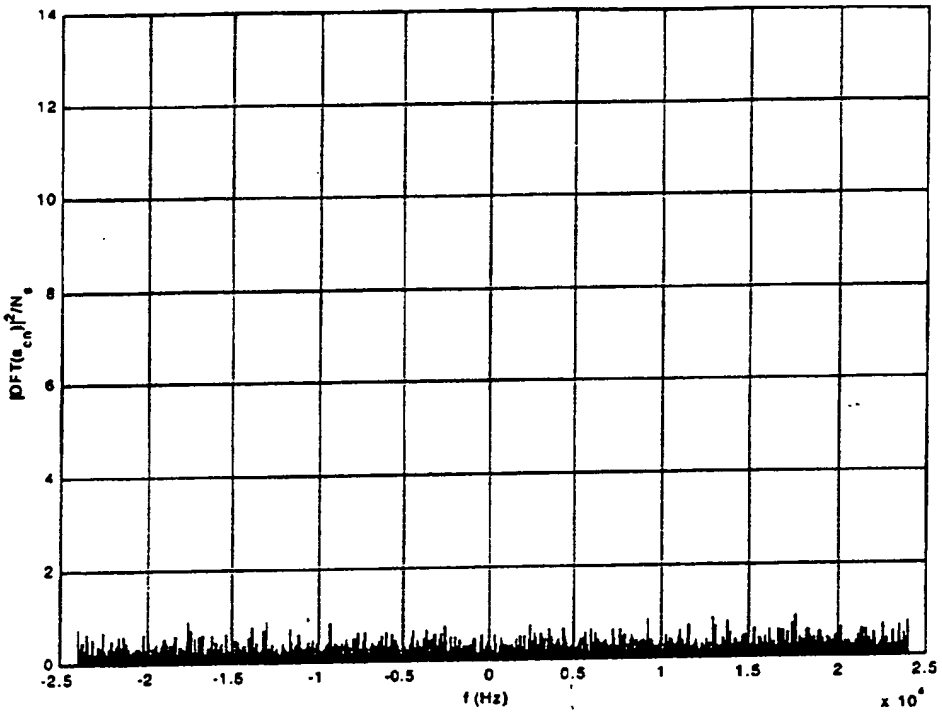

Figure 3

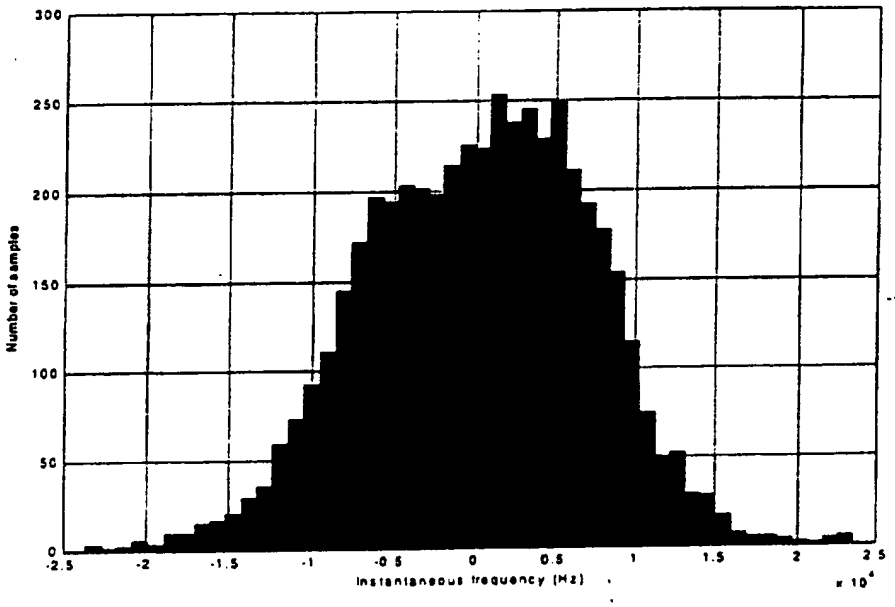
300
250
200
150
100
50
0
Number of samples
-2.5
-2
-1.5
-1
-0.5
0
0.5
1
1.5
2
2.5
Instantaneous frequency (Hz)
x 10^4

Figure 4

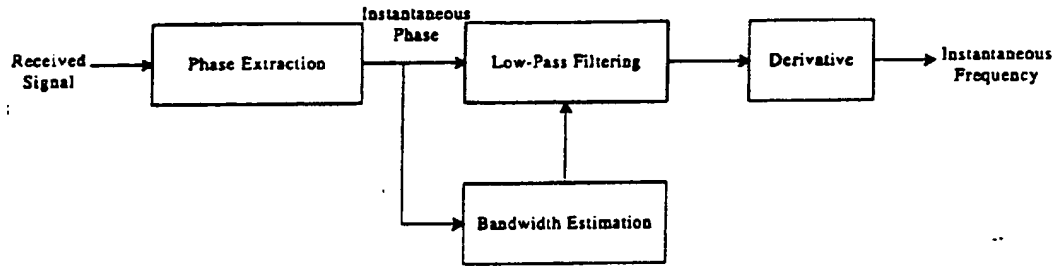
Received Signal
Phase Extraction
Instantaneous Phase
Low-Pass Filtering
Derivative
Instantaneous Frequency
Bandwidth Estimation

Figure 5

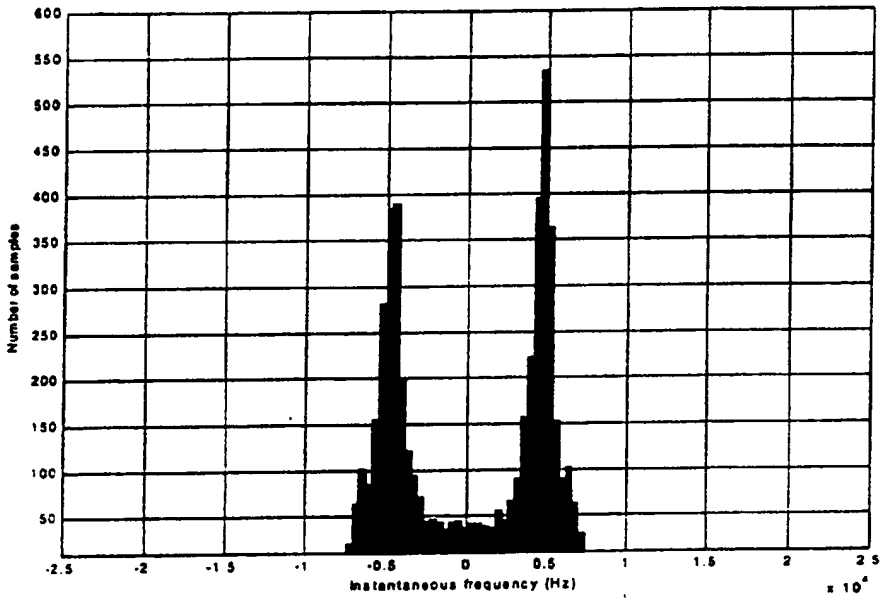
600
550
500
450
400
350
300
250
200
150
100
50
Number of samples
-2.5
-2
-1.5
-1
-0.5
0
0.5
1
1.5
2
2.5
Instantaneous frequency (Hz)
x 10^4

Figure 6

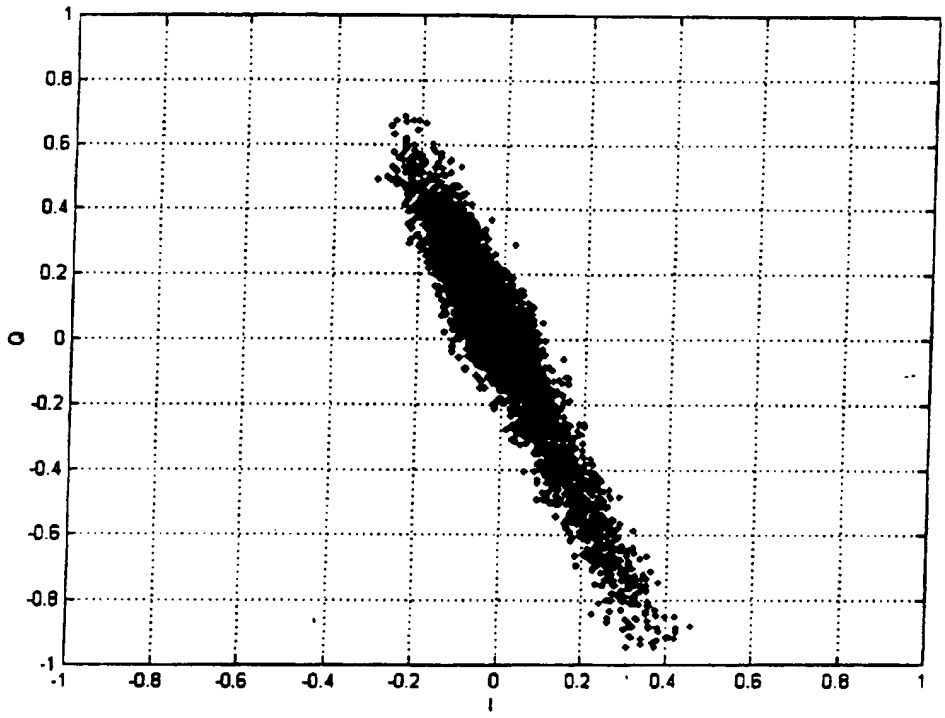

Figure 7

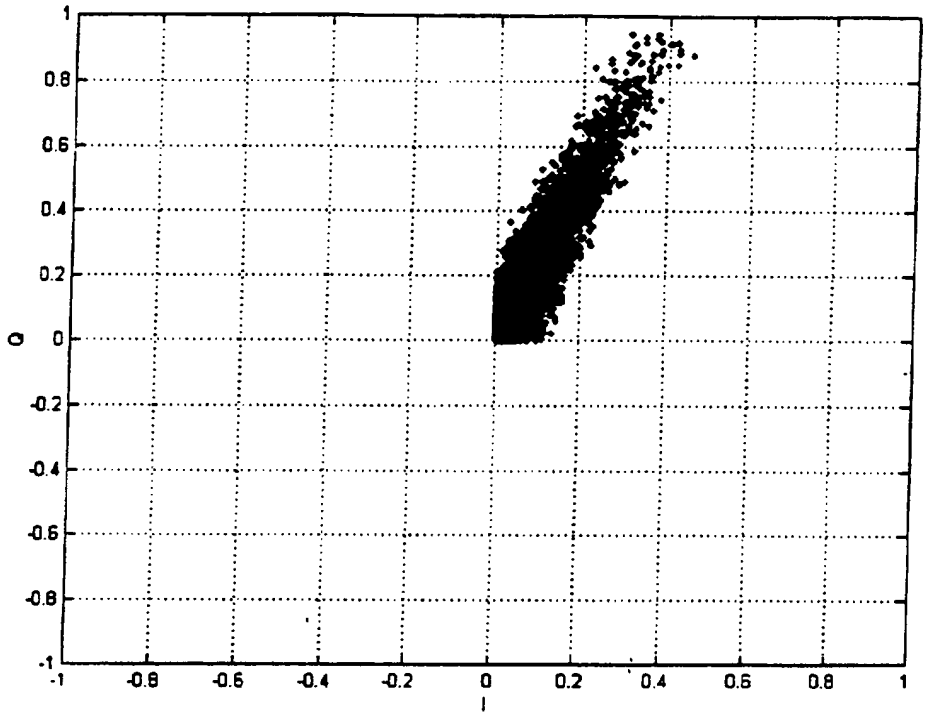

Figure 8

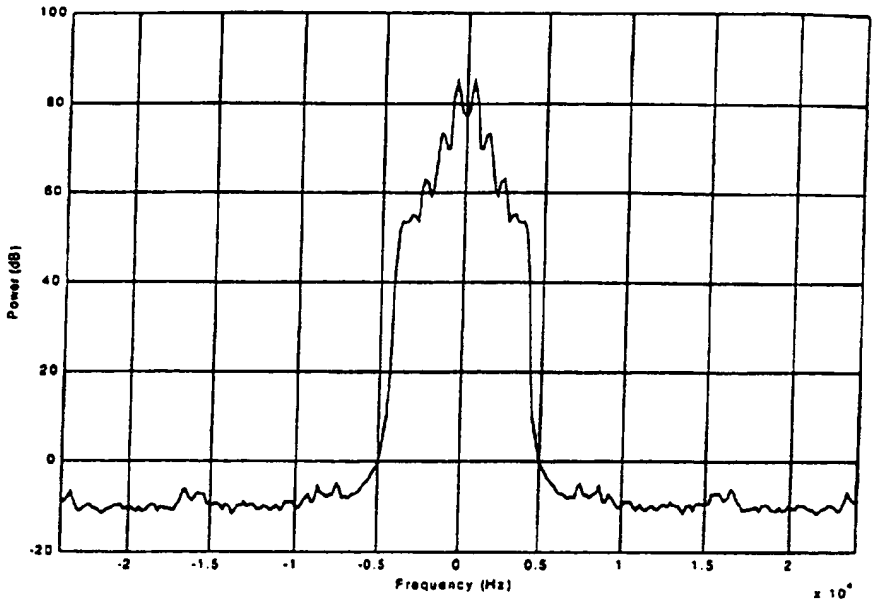

Figure 9

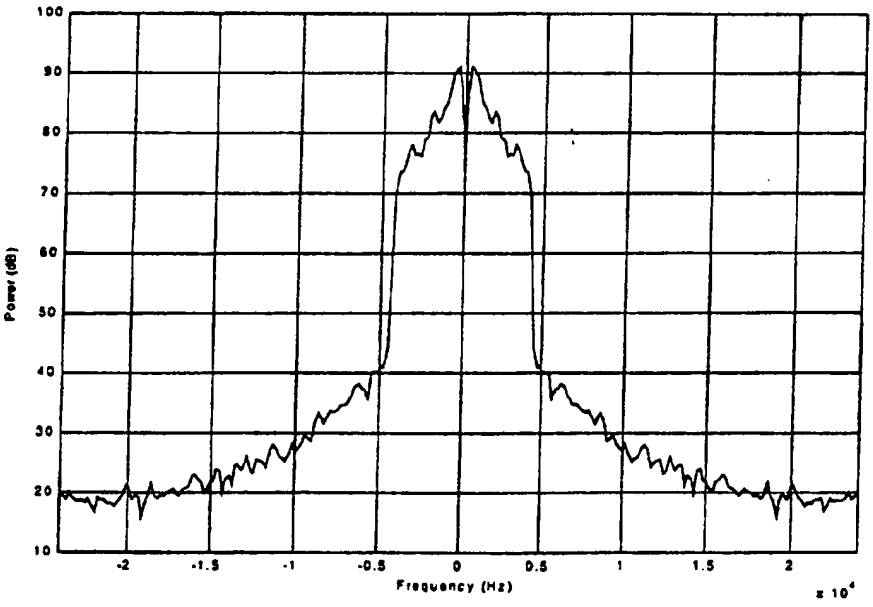

Figure 10

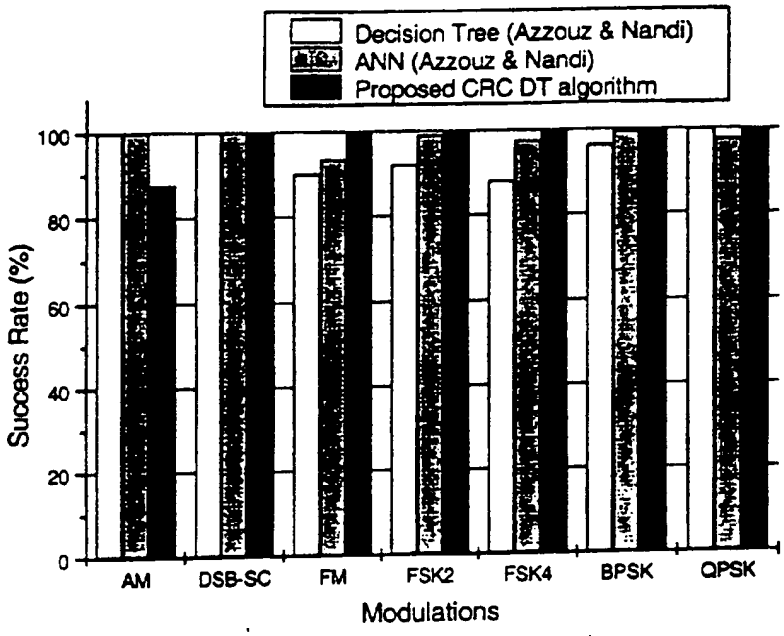
Decision Tree (Azzouz & Nandi)
ANN (Azzouz & Nandi)
Proposed CRC DT algorithm
Success Rate (%)
100
80
60
40
20
0
AM
DSB-SC
FM
FSK2
FSK4
BPSK
QPSK
Modulations

Figure 11

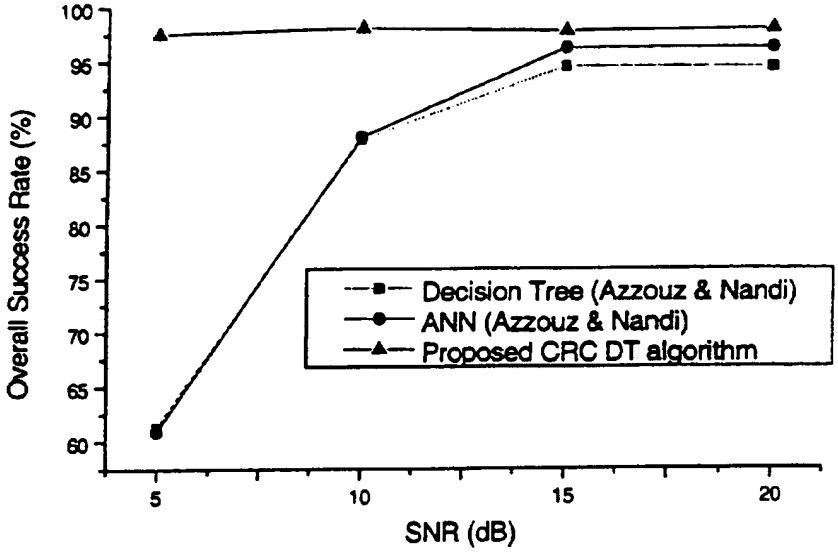
Overall Success Rate (%)
100
95
90
85
80
75
70
65
60
5
10
15
20
SNR (dB)
Decision Tree (Azzouz & Nandi)
ANN (Azzouz & Nandi)
Proposed CRC DT algorithm

Figure 12

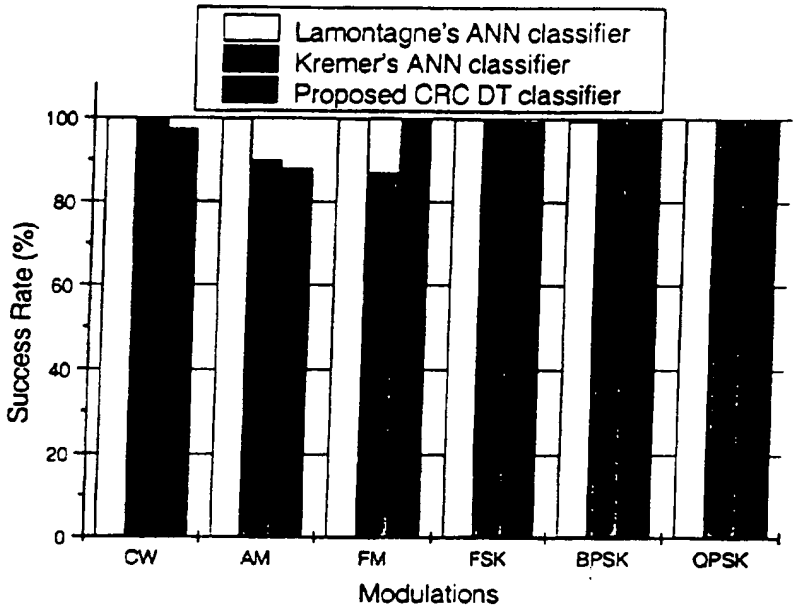
Lamontagne's ANN classifier
Kremer's ANN classifier
Proposed CRC DT classifier
Success Rate (%)
100
80
60
40
20
0
CW
AM
FM
FSK
BPSK
QPSK
Modulations

Figure 13

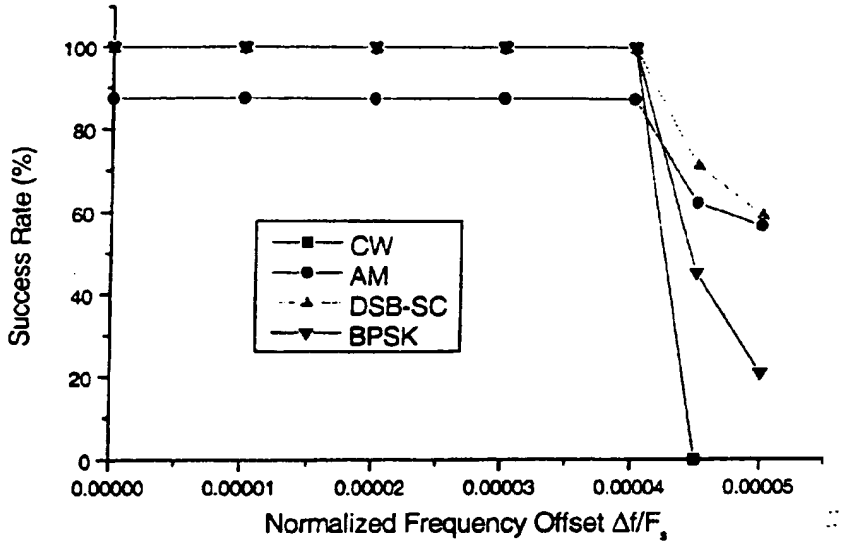

Figure 14

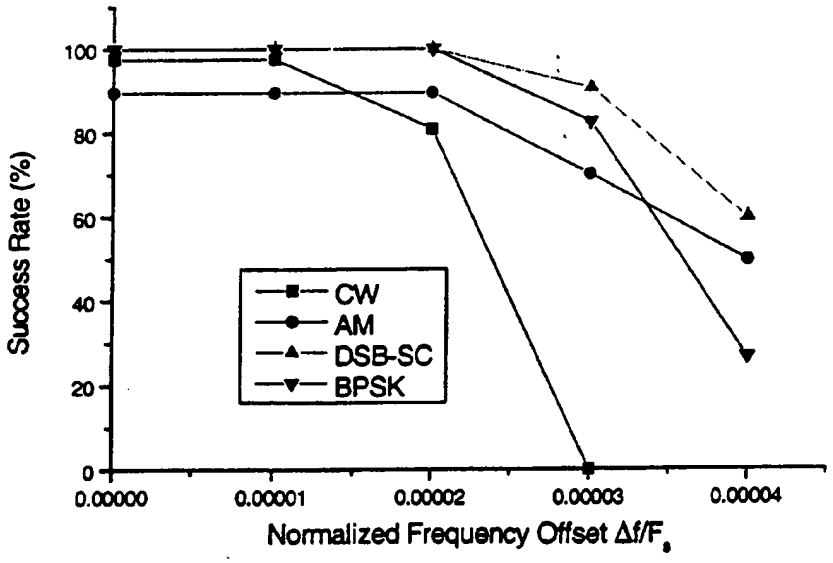

Figure 15

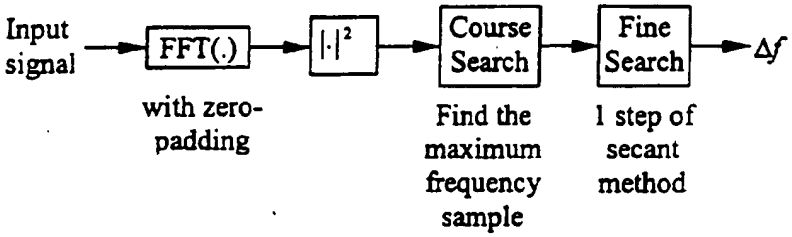
Input signal
FFT(.)
with zero-padding
$|\cdot|^2$
Course Search
Find the maximum frequency sample
Fine Search
1 step of secant method
Δf

Figure 16

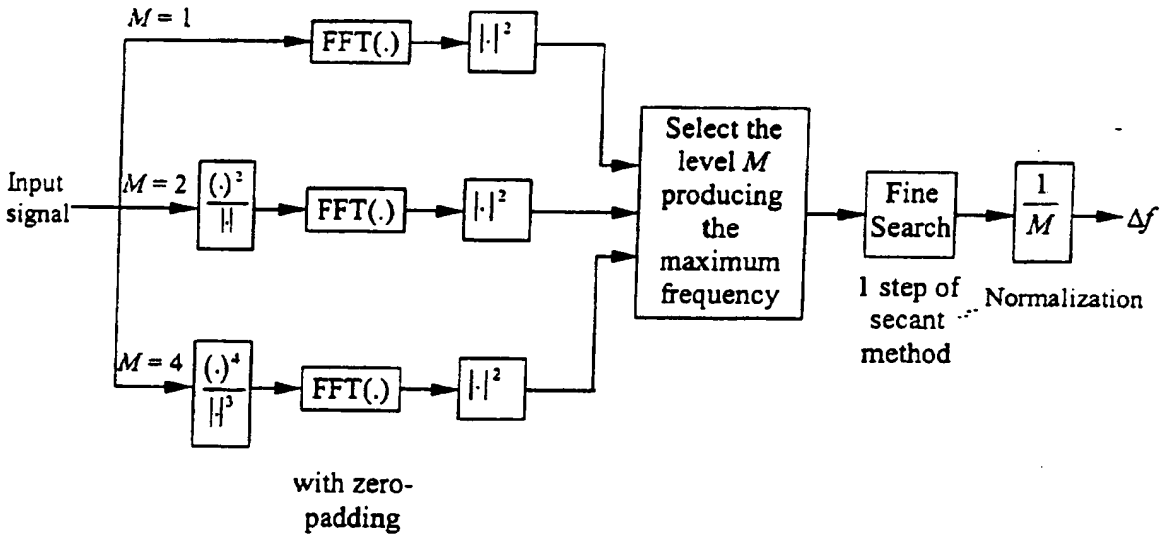
M = 1
FFT(.)
|.|²
Input signal
M = 2
(.)²/|.|
FFT(.)
|.|²
M = 4
(.)⁴/|.|³
FFT(.)
|.|²
with zero-padding
Select the level M producing the maximum frequency
Fine Search
1 step of secant method
1/M
Normalization
Δf

Figure 17

In the foregoing, it was assumed that the noise level was known. However, in practice, the variance of the noise must be estimated. Two methods are known in the art, the Level Crossing Rate (LCR) method and the Maximum Description Length (MDL) method.

In the spectrum monitoring context, several channels are observed by a wide-band channelisation receiver. The receiver requires knowledge of the noise floor in order to set a threshold that will produce a constant false alarm rate assuming the background noise has a normal distribution. For simplicity and speed, the receiver must detect the noise from a single FFT trace output. The length of the trace will vary since it is inversely proportional to the bandwidth of the narrowband channels being monitored. To ensure a fast scanning operation of the channelised receiver, it is important to minimise the number of points needed to extract the necessary information out of an FFT trace.

The frequency location and the presence of a signal may not be known by the monitoring equipment.

Very few techniques have been studied to address the general problem of noise floor or signal-to-noise ratio estimation [Aus95] [Pau95]. A typical approach is to isolate two channels, one with the desired signal and one with noise only, and then estimate the noise and signal power independently [Kel86]. Another typical approach is to assume that the signal dimension or signal location is known [Sto92]. In spectrum monitoring, these assumptions are difficult to meet because the channel allocation is changing, and the channels themselves are experiencing an on-off behaviour. Also, in general, it may not be possible to take the system off-line in an operational environment for periodical measurements. The conventional measurement procedure is lengthy and tedious and the noise floor is varying with the environmental conditions. According to the inventor's knowledge, only one implemented technique has been presented in the literature to do wide-band automatic noise floor estimation in the presence of signals [Rea97]. The technique is based on morphological binary image processing operators (similar to rank-order filtering) on a binary image of the received power spectrum. Thus it does not process the data directly, but the image of the spectrum. No precise performance results are presented in the paper. Also, no details are given with respect to the amount of data needed to get an estimate. It appears that the technique is computational intensive because it needs to generate a plot of the spectrum and to perform 2-D binary filtering. Techniques based on the idea of [Sto92] can also be used if an estimate of the signal dimension is provided. However, they would require many received vectors and result in a computationally complex procedure.

This application provides two techniques that operate on the frequency data to provide an estimate of the noise floor level. Performance in terms of occupancy and shape of the spectrum will be presented. The method is applicable to fast wide-band scanning.

Before going into the presentation of the two methods, a few definitions are given.

Measured Occupancy: The measured occupancy of a sequence composed of M elements is defined as the percentage (over M) of the elements above a given threshold corresponding to a probability of false alarm due to the noise floor power level.

True Occupancy: The true occupancy is the actual number of signals present in a spectrum bandwidth.

Noise floor power: The noise floor power level is the average power of the noise if no signals are present in a defined assignment band of a given region.

Channel bandwidth: The nominal channel bandwidth is the bandwidth of an assigned channel.

Signal occupied bandwidth: The signal occupied bandwidth is the bandwidth used by the channeliser to estimate the power in a given channel.

Level Crossing Rate (LCR)

The level crossing rate concept is used in wave propagation and communication channel modelling to obtain statistical information. The LCR is a second-order statistic that is time-dependent. It has mainly been use by Lee [Lee69][Lee82] in its work in mobile communications. The derivation of the level crossing rate for an analogue signal will follow.

Let a complex received signal $z(t)$ have uncorrelated real $x(t)$ and imaginary $y(t)$ components given by

$$z(t) = x(t) + jy(t) = e(t)e^{j\theta(t)}, \tag{1}$$

where $e(t)$ and $\theta(t)$ are the envelope (The squared envelope fluctuations are the same) and the phase of $z(t)$ given by

$$\begin{aligned} e(t) &= \sqrt{x(t)^2 + y(t)^2} \\ \theta(t) &= \tan^{-1}\left(\frac{y(t)}{x(t)}\right). \end{aligned} \tag{2}$$

The derivative $\dot{z}(t)$ of $z(t)$ with respect to t is

$$\dot{z}(t) = \frac{dz(t)}{dt} = \dot{x}(t) + j\dot{y}(t). \tag{3}$$

In [Lee82], it is proven that the four random variables $x(t)$, $y(t)$, $\dot{x}(t)$ and $\dot{y}(t)$ are independent real Gaussian random variables with joint probability density function given by

$$p[x(t), y(t), \dot{x}(t), \dot{y}(t)] = \frac{1}{(2\pi)^2\sigma^2\rho^2}\exp\left[-\frac{1}{2}\left(\frac{x^2(t)+y^2(t)}{\sigma^2} + \frac{\dot{x}^2(t)+\dot{y}^2(t)}{\rho^2}\right)\right], \tag{4}$$

where σ^2 and ρ^2 are the variance of the real and imaginary part of $z(t)$ and $\dot{z}(t)$ respectively. In terms of the derivative of the $e(t)$, it is also shown in [Lee82] that

$$\begin{aligned} x(t) &= e(t)\cos[\theta(t)] \\ y(t) &= e(t)\sin[\theta(t)] \\ \dot{x}(t) &= \dot{e}(t)\cos[\theta(t)] - e(t)\dot{\theta}(t)\sin[\theta(t)] \\ \dot{y}(t) &= \dot{e}(t)\sin[\theta(t)] + e(t)\dot{\theta}(t)\cos[\theta(t)] \end{aligned}$$

Applying a change of variable, the joint probability density function of $e(t)$, $\theta(t)$, $\dot{e}(t)$ and $\dot{\theta}(t)$ is given by

$$p[e(t),\theta(t),\dot{e}(t),\dot{\theta}(t)]=\frac{e^2(t)}{(2\pi)^2\sigma^2\rho^2}\exp\left[-\frac{1}{2}\left(\frac{e^2(t)}{\sigma^2}+\frac{e^2(t)\dot{\theta}^2(t)+\dot{e}^2(t)}{\rho^2}\right)\right]. \quad (5)$$

After the integration of $\theta(t)$ and $\dot{\theta}(t)$ from 0 to 2π and $-\infty$ to ∞ respectively, we obtain

$$p(e(t),\dot{e}(t))=\frac{e(t)}{\sqrt{2\pi\rho^2}\sigma^2}\exp\left[-\frac{1}{2}\left(\frac{e^2(t)}{\sigma^2}+\frac{\dot{e}^2(t)}{\rho^2}\right)\right]. \quad (6)$$

The level crossing rate is the total number of crossing per second of a signal at a given threshold. It is given by

$$n[e(t)=A]=\int_0^\infty \dot{e}(t)p[e(t),\dot{e}(t)]d\dot{e}(t)=\frac{\rho A}{\sqrt{2\pi\sigma^2}}\exp\left(-\frac{A^2}{2\sigma^2}\right). \quad (7)$$

If the normalised level R defined as $R = A/\sqrt{2\sigma^2}$ is used than we have

$$n\left[\frac{e(t)}{\sqrt{2\sigma^2}}=R\right]=\frac{\rho R}{\sigma\sqrt{\pi}}\exp\left(-R^2\right). \quad (8)$$

The variance $R_{\dot{z}(t)\dot{z}(t)}(0)=2\rho^2$ of the derivative process $\dot{z}(t)$ is given in general by

$$R_{\dot{z}(t)\dot{z}(t)}(0)=-\left.\frac{d^2R_{z(t)z(t)}(\tau)}{d\tau^2}\right|_{\tau=0}. \quad (9)$$

The LCR function in (8) is illustrated in

Figure 3 for several values of the parameter α of the autocorrelation function $R_{z(t)z(t)}(\tau)=\sigma^2\exp\left(-\alpha^2\tau^2\right)$. For this function we have $\rho^2=2\alpha^2\sigma^2$. Note that the peak of the function is located at –3 dB from the actual variance of the data. It can thus be used to estimate the noise floor power when most of the signal is noise. As well, it is observed that the LCR value decreases as the correlation parameter $1/\alpha$ increases.

List of Figures

Maximum Description Length (MDL)

Let's assume that the known covariance matrix $\mathbf{R}$ of N FFT trace output vector $\mathbf{y}_n$, $n = 1, 2, \ldots N$, of length MK is of the form

$$E\{\mathbf{y}_n \mathbf{y}_n^H\} = \mathbf{R} = \mathbf{S} + \sigma^2 \mathbf{I}, \tag{10}$$

where $\mathbf{S}$ is the covariance matrix of the signal components, σ^2 is the variance of the additive complex white Gaussian noise in the frequency domain, and $\mathbf{I}$ is a unitary diagonal matrix. The matrix $\mathbf{S}$ can be decomposed into a quadratic form as

$$\mathbf{S} = \mathbf{V}\Lambda\mathbf{V}^H, \tag{11}$$

where $\mathbf{V}$ is a matrix with columns eigenvector $\mathbf{v}_k$ associated with the k-th element on the diagonal matrix Λ, the eigenvalue λ_k. If we assume that the number of signals q in $\mathbf{S}$ is smaller than MK, than it is readily apparent that the last $MK - q$ eigenvalues. of $\mathbf{R}$ will be

equal (the eigenvalues of **R** are given by $\lambda_k + \sigma^2$) to σ^2. The number of signal can thus be estimated. For our application, the matrix **R** is not known and must be estimated. When estimated from a finite sample size, the resulting eigenvalues are all different with probability one, thus making it difficult to determine the number of signals merely by observing the eigenvalues.

Suppose it is assumed that the signal dimension is $k \le MK$. The parameter vector of the model would then be $\Theta^{(k)} = \left(\lambda_1, \cdots, \lambda_k, \sigma^2, \mathbf{v}_1^T, \cdots, \mathbf{v}_k^T\right)^T$ with the eigenvalues and eigenvectors of the covariance matrix $\mathbf{R}^{(k)}$. This matrix can thus be expressed as [Max85]

$$\mathbf{R}^{(k)} = \sum_{i=1}^{k} \left(\lambda_i - \sigma^2\right) \mathbf{v}_i \mathbf{v}_i^H + \sigma_w^2 \mathbf{I}_K . \tag{12}$$

Under the assumption that the vectors $\mathbf{y}_n$ are statistically independent, the joint probability density function of the N vectors is

$$p\left(\mathbf{y}_1, \cdots, \mathbf{y}_N \middle| \Theta^{(k)}\right) = \prod_{n=1}^{N} \frac{1}{\pi^{MK} \det \mathbf{R}^{(k)}} \exp\left[-\mathbf{y}_n^H \mathbf{R}^{(k)-1} \mathbf{y}_n\right]. \tag{13}$$

Taking the logarithm and omitting terms that do not depend on the parameter vector $\Theta^{(k)}$, the log-likelihood function $L(k)$ is given by

$$L(k) = \ln\left[p\left(\mathbf{y}_1, \cdots, \mathbf{y}_N \middle| \Theta^{(k)}\right)\right] = -N \ln \det \mathbf{R}^{(k)} - N \operatorname{tr}\left(\mathbf{R}^{(k)-1} \hat{\mathbf{R}}\right), \tag{14}$$

with

$$\hat{\mathbf{R}} = \frac{1}{N} \sum_{n=1}^{N} \mathbf{y}_n \mathbf{y}_n^H . \tag{15}$$

The maximum likelihood estimate is the value of $\Theta^{(k)}$ that maximises (14). These estimates are given by [Max85]

$$\hat{\lambda}_i = l_i, \quad i = 1, \cdots, k; \tag{16}$$

$$\hat{\sigma}_w^2 = \frac{1}{K-k} \sum_{i=k+1}^{K} l_i ; \tag{16a}$$

$$\hat{\mathbf{v}}_i = \mathbf{c}_i, \quad i = 1, \cdots, k; \tag{16b}$$

where $l_1 > l_2 > \ldots > l_{MK}$ and $\mathbf{c}_1, \ldots, \mathbf{c}_{MK}$ are the eigenvalues and eigenvectors of (15). Substituting (16) in (14) and removing the constant terms, it is found that

$$L(k) = N \ln \left[\frac{\prod_{i=k+1}^{K} l_i}{\left(\frac{1}{K-k} \sum_{i=k+1}^{K} l_i \right)^{K-k}} \right], \; k = 0, 1, \ldots, MK - 1. \tag{17}$$

The MDL criteria estimate of q is then defined as the value of k that minimises $-L(k)$ plus a penalty function related to the number of free parameters in the model $\Theta^{(k)}$. In mathematical terms it is defined as

$$\hat{q}_{MDL} = \arg\min_k \left\{ -L(k) + \frac{k}{2}(2MK - k)\ln N \right\}. \tag{18}$$

The index $\hat{q}_{MDL}$ is the dimension of the signal space. Thus to estimate the noise variance it is sufficient to compute

$$\hat{\sigma}^2 = \frac{1}{MK - \hat{q}_{MDL}} \sum_{i=\hat{q}_{MDL}+1}^{MK} l_i. \tag{19}$$

These prior art concepts presented above are general and are not readily applicable to the noise floor estimation for wide-band FFT filter bands. They need to be modified or refined to fit with the particularity and the practicality of the real world system.

The present invention now provides methods that are implemented in a real-time system. One problem with the known LCR is that it is not intended for use with a finite discrete-frequency sequence. To overcome this difficulty, the present invention provides a method which uses a histogram with quantised decibel values. Thus the first step is to compute the logarithm values of the envelope squared of the complex FFT values at the output of the filter bank. The exact analysis of the quantized data is difficult because of the non-linearity of the operation. To demonstrate that approach still leads to an estimate of the actual noise floor level, the analogue signal will be used. Later, examples of the discrete approach will be presented.

The squared amplitude of the filter bank complex values result in a random variable Y having an exponential probability density function when only a noise signal is present. Taking the logarithm base 10 and multiply by 10 results in a new random variable called $Z = 10\log_{10} Y$ with a probability density function given by

$$p_Z(z) = \frac{10^{z/10}}{20\sigma^2 \log_{10} e} \exp\left(-\frac{10^{z/10}}{2\sigma^2} \right), \tag{20}$$

with z going from $-\infty$ to ∞. Following the procedure in section 0 where $e(t)$ is now replaced by Z, and knowing that it has been shown in [Ric48] that for most wide processes, the derivative of Z is independent of Z and Gaussian. The joint probability $p_{Z\dot{Z}}(z, \dot{z})$ of the process is found to be

$$\begin{aligned} p_{Z\dot{Z}}(z, \dot{z}) &= p_Z(z) p_{\dot{Z}}(\dot{z}) \\ &= \frac{10^{z/10}}{20\sigma^2 \log_{10} e} \exp\left(-\frac{10^{z/10}}{2\sigma^2} \right) \frac{1}{\sqrt{2\pi}\rho} \exp\left(-\frac{\dot{z}^2}{2\rho^2} \right). \end{aligned} \tag{21}$$

To evaluate the LCR, it suffices to use (21) with the formal definition of the LCR, i.e.,

$$n[Z = A] = \int_0^\infty \dot{z} p_{Z\dot{Z}}(z, \dot{z}) d\dot{z}$$

$$= p_Z(z) \int_0^\infty \dot{z} p_{\dot{Z}}(\dot{z}) d\dot{z}$$

$$= \frac{\rho 10^{A/10}}{20\sigma^2 \log_{10} e} \exp\left(-\frac{10^{A/10}}{2\sigma^2}\right). \quad (22)$$

The function (22) has a single maximum that can easily be verified to be located at $10\log_{10}(2\sigma^2)$. The main difficulty in (22), is to evaluate ρ, the standard deviation of the derivative of the logarithm of the envelope squared. The value will depend on the auto-correlation function of the envelope process, thus on the window choice. However in the present context, this value is not really needed since the value of σ^2 is not even known in the first place. The important parameter to estimate is the value of σ^2 and it can be estimated with the position of the maximum of the function.

The expression (22) is for a continuous-time signal. To deal with discrete-time signals and to ease implementation, (22) is approximated by quantizing the measured dB values to the nearest integer value and to build a histogram of the number of occurrences of the crossing of the integer dB values. This procedure produces a function having a shape very similar to (22) when only noise is present. When a large number of modulated signals are present, the global maximum may not be the estimate of the noise power. Figure 1 is showing the discrete LCR curves for two scenarios ([1] Note that the average normalised number of occurrence per FFT vector is dependent also on the window choice.) of channel occupancy, with the function (22) with noise only.

The noise power estimate per bin for the noise only scenario is –9 dB while when the band is occupied at 75 percent, it would be 15 dB if the global maximum is selected. To avoid this wrong behaviour, the first local maximum from the right side is selected. To ensure that no greater local or global maxima are close to this local maximum, it is then verified that there is no greater maximum on the left side closer to Y dB.

Accordingly the method of the invention comprises the steps of:

1) Computing an FFT amplitude trace output in dB, of an input complex vector,
2) Quantising the dB value to the nearest integer dB value,
3) Creating an empty histogram with bins from a minimum value to a maximum value, of the quantised B values,
4) For every positive slope segment of the quantised trace, adding a 1 to the histogram bin that is crossed by the curve, except the end point of the positive curve segment,
5) Finding the first local maximum of the histogram starting from the minimum quantised dB value,
6) Checking if an other local maximum is present Y=Z higher than the current maximum: if no, than the current maximum abscissa is the noise floor level per bins; if yes, going to that maximum and applying 6) again until the answer is no.

7) Finding the noise floor per channel by applying the dB correction of

dB value of noise floor per bin + 10 $\log_{10}$(number of used bin per channel) + 3.

The method performs very well when the number of bins per channel and the number of channels per FFT trace are large and when the occupancy level is relatively low.

There are two problems with the MDL of the art. The first one is that it requires a large number (larger or equal to the number of channels times the number of bins per channel) of FFT trace outputs to form a covariance matrix. In a fast channelisation receiver, this is unacceptable. Secondly, it requires an eigen-decomposition of a large matrix. This is a complex operation that is likely to increase significantly the processor load. Thus is must be avoided. Also, it requires a sort function on the eigenvalues which is also a complex operation. These problems are now overcome with, a simplified MDL method in accordance with the invention.

The first requirement is that the noise power level be determined from a single FFT trace. To avoid the sort operation, the squared FFT coefficients of a trace are transformed in dB values and then quantised to the nearest integer values. This operation is needed anyway. The interger values are then put in an histogram and subsequently extracted from the histogram by group of K, the number of bins per channel. This is effectively the equivalent of a sort function and a very good approximation to the true sort operation. It also reduces the side of the problem from MK to M. An other impact of the operation is that the sample power will tend to be decorrelated even with a window because they are now from non adjacent bins. Next as in the case of the MDL, these M points corresponding to the power of K bins in decreasing order are used in the log-likelihood function of (14). The penalty function $p(k)$ is subtracted from the log-likelihood function to form the criteria over which the minimum will be searched. The penalty function however in this case is a different polynomial function compared to the one of the prior MDL. The reason for the change is due to the fact that the method of the invention does not need to account for the eigenvectors, thus reducing the penalty of interested is only the amplitude of the equivalent of the eigenvalues. Thus when $k = 0$, we have MN free parameters, when $k = 1$, we have $(M - 1)N$ free parameters and so on. The penalty function is however a second order polynomial. It was determined by examining the log-likelihood function when only noise is present and fitting a polynomial function. This polynomial function is then scaled to avoid erroneous detection due to the variance in the data. Thus the only assumption here is that the FFT coefficients have a Gaussian distribution which should be valid since they result from a linear combination of variables that are Gaussian. If the sample data are not normal, the linear combination will then transform then in Gaussian variables. The scale factor gives a degree of freedom in the optimisation process. Figure 2 illustrates the log-likelihood function and the fitting function. The actual function that is minimised is

$$\hat{q}_{NF} = \arg\min_{k}\{-L(k) + Cp(k)\}. \qquad (23)$$

In another aspect, the invention provides a method including the steps of:

1) Building a histogram from a FFT output trace quantized to the nearest integer dB value,
2) Transforming the histogram into a sorted linear vector,

3) Chanelizing the sorted linear vector into M groups, by summing the samples of the sorted vector,
4) Applying the log-likelihood function on the sorted group, of M elements
5) Adding the penalty polynomial function to the negative of the log-likelihood,
6) Finding the index of the global minimum, and
7) Estimating the noise floor as the average of the last M minus the index number smallest sorted groups.

The performance of both methods in accordance with the invention is a very important factor but it must also be weighed against the complexity of the approaches. The starting point will be the MK values of the complex squared FFT coefficients and the stopping point will be after the noise floor estimate per FFT bin. The complexity will be measured by counting the number of multiply, add, compare and math functions.

Table 1 summarises the operations for both methods. From that table we conclude that both methods are approximately of the same complexity. Both methods operate on the bin basis and can provide the noise floor per bin or channel. Both methods are dominated by the compare operations.

Table 1. Complexity comparison of the discrete LCR and simplified MDL.

	LCR	MDL	LCR ($M=256, K=8$)	MDL ($M=256, K=8$)
$\times$ /	MK	$MK+6M$	2048	3584
+ –	$2MK$	$MK+4M$	4096	3092
$\log_{10}$ or $\log_e$	MK	$MK+M$	2048	2304
Compare	$\approx 3MK+60$	$2MK+M$	6204	4352
Round	MK	MK	2048	2048
$(\bullet)^a$	0	$\approx M+60$	0	316
Total	$\approx 8MK$	$\approx 13\,MK+13\,M$	16444	15696

Example I

To evaluate the respective performances of both methods, a simulation program and a real-time implementation were written to estimate the mean and variance of the noise floor level computed by the LCR and MDL. The mean value of the estimate will indicate if a bias is present and its size in the algorithms while the variance will indicate the stability of the estimate.

The transmitted signals used for the simulation are a binary FSK signal similar to a Jaguar radio (20 kbps data rate instead or 19.2 kbps for the Jaguar radio), and a measured FM signal in the 139 to 144 MHz band. The channel bandwidth is 25 kHz for the binary FSK signal and 15 kHz for the FM signal. The windowed FFT filter bank is using a Blackman window. To reduce the amount of simulation results to present, the number of channel M has been limited to 64 and the number of bin per channel K to 8. These numbers are typical of what is expected in practice. Table 2 presents the results for other choices of M and K for an

occupancy level of 50 % and the equal carrier power pattern, where it is apparent that for $K \geq 4$, the results do not change very much as a function of M and K.

Table 2. Mean estimate value for 50 % occupancy of jaguar signals with equal carrier power at 20 dB above 0 dB noise floor.

K	$M = 16$	$M = 64$	$M = 256$
1	MDL = 51.5; LCR = 68.2	MDL = 47.5; LCR = 37.5	MDL = 48.5; LCR = 47.6
2	MDL = 27; LCR = 29.4	MDL = 10.4; LCR = 7.93	MDL = 3.07; LCR = 12.7
4	MDL = 1.4; LCR = 4.7	MDL = 1.01; LCR = 1.3	MDL = 1.05; LCR = 1.93
8	MDL = 1.12; LCR = 1.14	MDL = 1.13; LCR = 1.35	MDL = 1.16; LCR = 1.56
16	MDL = 1.17; LCR = 1.12	MDL = 1.17; LCR = 1.39	MDL = 1.2; LCR = 1.47

The results of the estimators are presented for occupancy level of 0 % to 93.75 % with four different carrier power patterns. They are referred to as equal power (dBe), ramp power (dBr), ramp and equal power (dBer), and equal and ramp power (dBre). The typical shapes are illustrated in Figure 4. These are the pattern if the carrier power were sorted. In the simulation, the amplitudes are assigned random frequency locations multiple of the channel bandwidth. The results are illustrated in Figure 5 to Figure 9 for the best parameters of the two methods for the four power patterns of Figure 4. From the above results, it is apparent that both methods have less than a 3 dB bias error at up to about 60% occupancy. The bias could potentially be removed since it is possible to have an estimate of the occupancy on the trace. The bias appears because the Jaguar signal (binary FSK signal) is a difficult signal in the sense that it fills its 25 kHz assigned bandwidth completely (see Fig. 16). For signals where a guard band is present, the performance will in general be even better than shown in Fig. 5 for the most difficult cases of an FM signal, i.e. equal carrier power level. From these sets of results, it is concluded that the LCR has slightly better general performance but with a larger variance than the MDL. For the FM signal, the MDL seems to have an advantage. Next Fig. 10 presents the time variations of the estimates of the two methods for 50% occupancy for 64 channels and 8 bins/channel with the binary FSM signal. A conclusion from these figures is that time averaging of the noise level estimate will be necessary to limit the false detection rate. This should not be a problem since the noise process is usually a very slow varying process.

FM signal at 20 dB SNR with equal power levels.

Example II

DAS Measurements

The results of the previous section were indicative of the bias and the variance in the estimators. The objective in the estimation of the noise floor is to derive the threshold level for detection. This section presents results on the average probability of false alarm of the unused channels $\overline{P_{fa}}$ and the probability of detection P_d of one channel for the two noise floor level estimation methods, and for the known noise floor level as a comparison. The desired signal is at the maximum power level of the power pattern. The impact of the estimator's variance are assessed for the equal-ramp power pattern as a function of the time average of the estimate, the occupancy level, and the signal-to-noise ratio. The signal-to-noise ratio is

defined as the amplitude square of the transmitted signal over the noise variance in the nominal channel bandwidth. For a given occupancy level, the power pattern is fixed and relative to the maximum SNR, i.e. 30 dB. This means that as the SNR increases, more channels are visible out of the noise floor. The synthesised signal is a BFSK radio in a 25 kHz spacing with $M = 64$ channels, $N = 6$ bins used for detection out of $K = 8$ bins in the detection process, a desired $P_{fa} = 10^{-3}$, and number of averages of 1, 10, and 100 estimates. The results are illustrated in Figures 11 to 15.

Figure 11 shows that $\overline{P}_{fa}$ increases as a function of the SNR and the occupancy for the known SNR case. This is not a surprise since the transmitted signal causes adjacent channel interference. The occupancy level does not affect the probability of detection. For the noise floor estimators now, Figure 12 presents the probabilities when the instantaneous values of the estimators are used in the threshold. The LCR has an order of magnitude increase in its $\overline{P}_{fa}$ relative to the desired value. The MDL is close to 10^{-3} for low occupancies but is below for moderate and high occupancy for the range of SNR below 20 dB. This is indicative that the algorithm over-estimates the noise floor level. The probability of detection decreases as a function of occupancy and the LCR seems to provide a few fraction to a few dB of advantage over the MDL in the SNR range from 0 to 12 dB. Figure 13 is for the same scenario as Figure 12 except that 10 averages are used instead of 1. The behaviour of P_d is similar to the case of a single average of the noise floor estimate. The average probability of false alarm of the unused channels of the LCR and MDL is now similar with the LCR values being higher in the range of SNR up to approximately 22 dB. The results of averaging 100 estimates are presented in Figure 14 and they are basically the same as Figure 13. This means that averaging 10 estimates is sufficient to guarantee a "normal" behaviour compared to the known SNR case. Finally, Figure 15 presents the results for the FM signal were it is seen that in the absence of weak adjacent channel interference, the difference between the known channel SNR and the estimated noise floor performances are negligible.

It should be pointed out that for strong signals, the probability of false alarm of unused channels is always larger than the desired value. These results should be taken into account in the detection algorithm or in a database storing the power results for further analysis.

The following parameters are preferred for carrying out the first version of the noise floor estimation: Implement the LCR algorithm with 2 dB look over,

a) A window of 10 estimates is sufficient to reduce the time variation of the estimate to an acceptable level of probability of detection degradation,

b) Measure the LCR performance in terms of variance and bias as a function of the measured occupancy (estimated with a threshold),

c) Implement and test the MDL in a test version (in the DAS or in Matlab) to verify the observation that it performs well with real life signals (Figure 9 and Figure 15)

d) Investigate the possibility of reducing the complexity of the algorithms.

These recommendations together with the results of the measurements should then indicate if further refinements to reduce the bias as a function of occupancy are really needed for real life signals. Also, a mechanism to indicate the failure of the algorithm should be developed so that bad estimation should be marked.

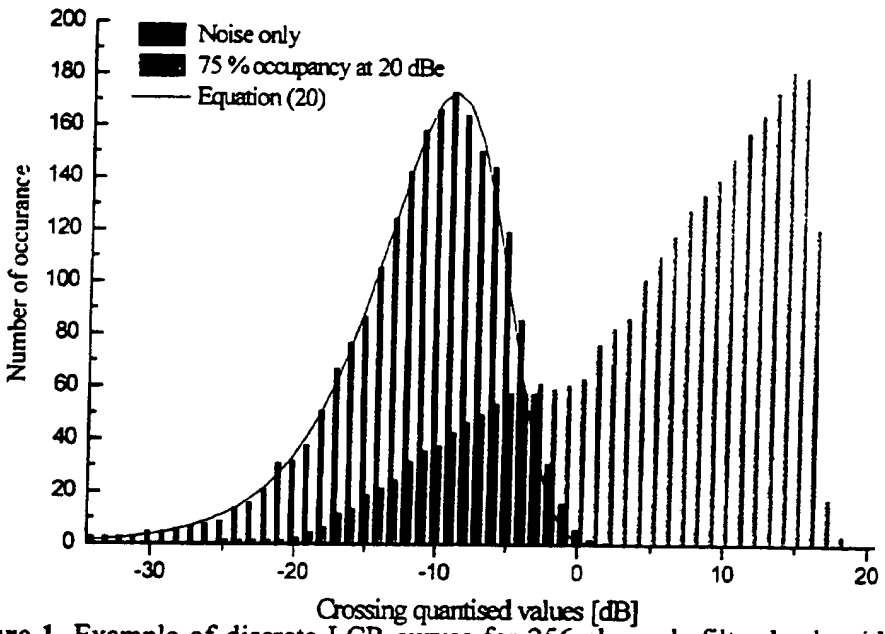

Figure 1. Example of discrete LCR curves for 256 channels filter bank with 4 bins per channel with a Blackman window.

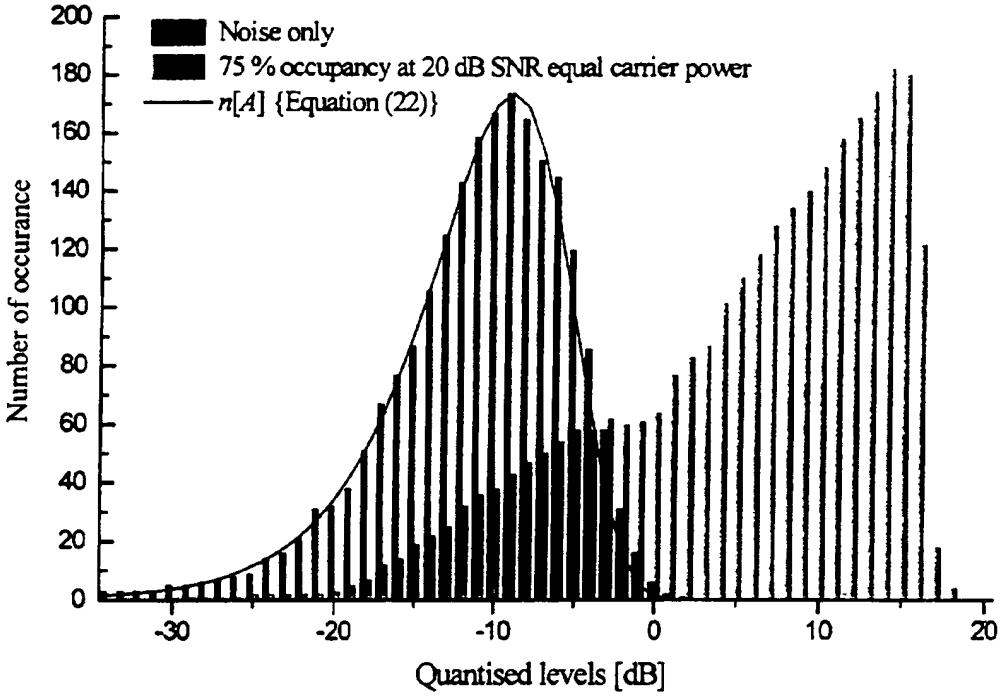

Figure 2. Normalised log-likelihood function and polynomial fit with noise only for $M = 64$ and $K = 8$.

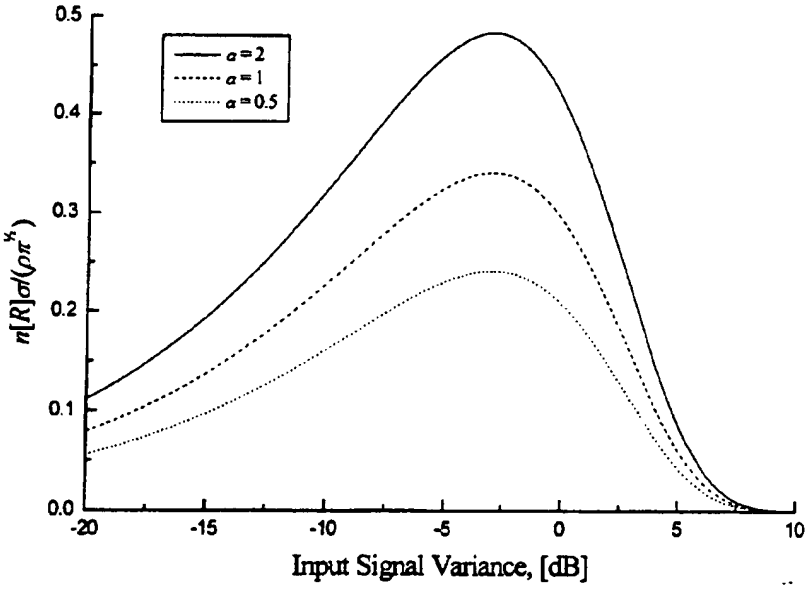

Figure 3. Normalised LCR curve for the complex Gaussian noise only signal.

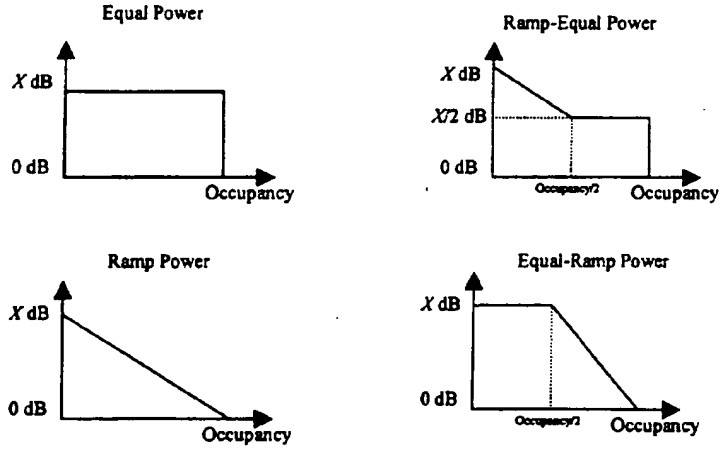

Figure 4. Pattern of carrier signal power.

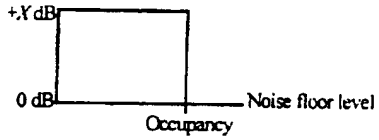

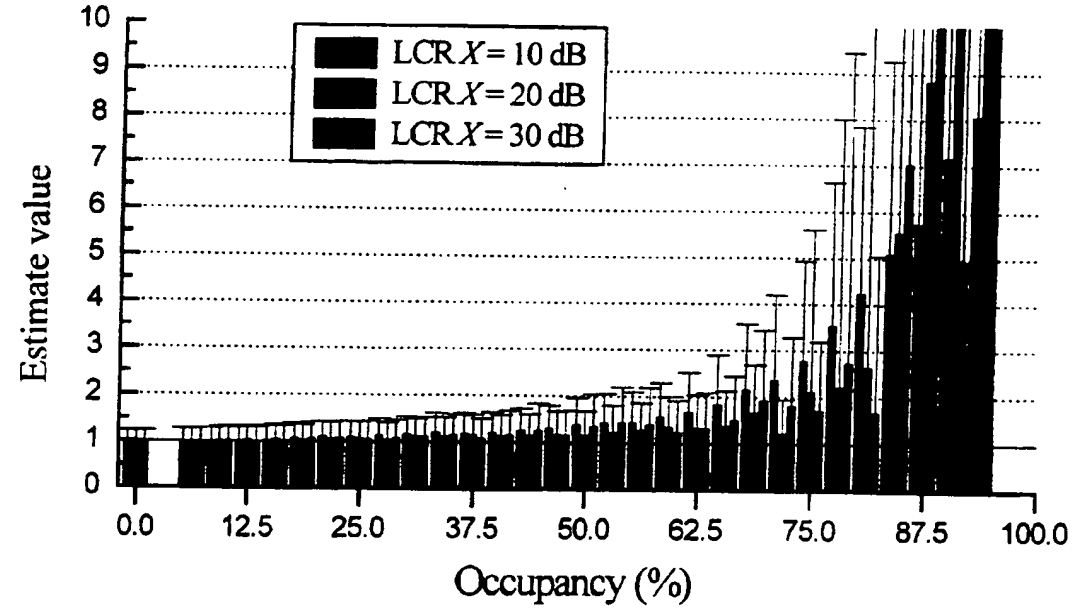

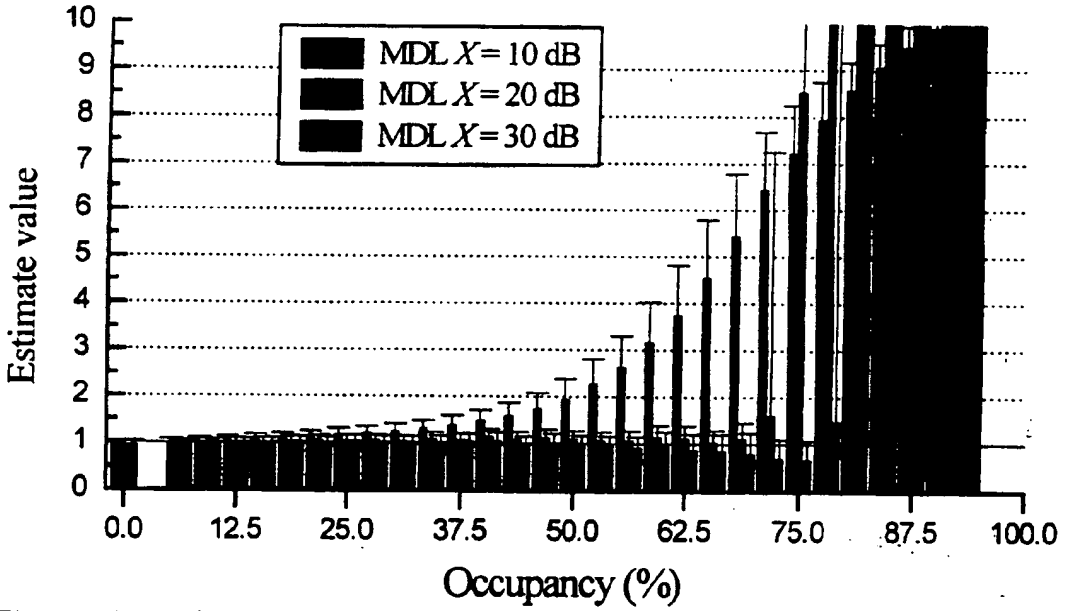

Figure 5. Noise floor level estimation for dBe power, $K = 8$, $M = 64$, and BFSK signal.

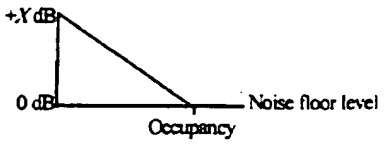

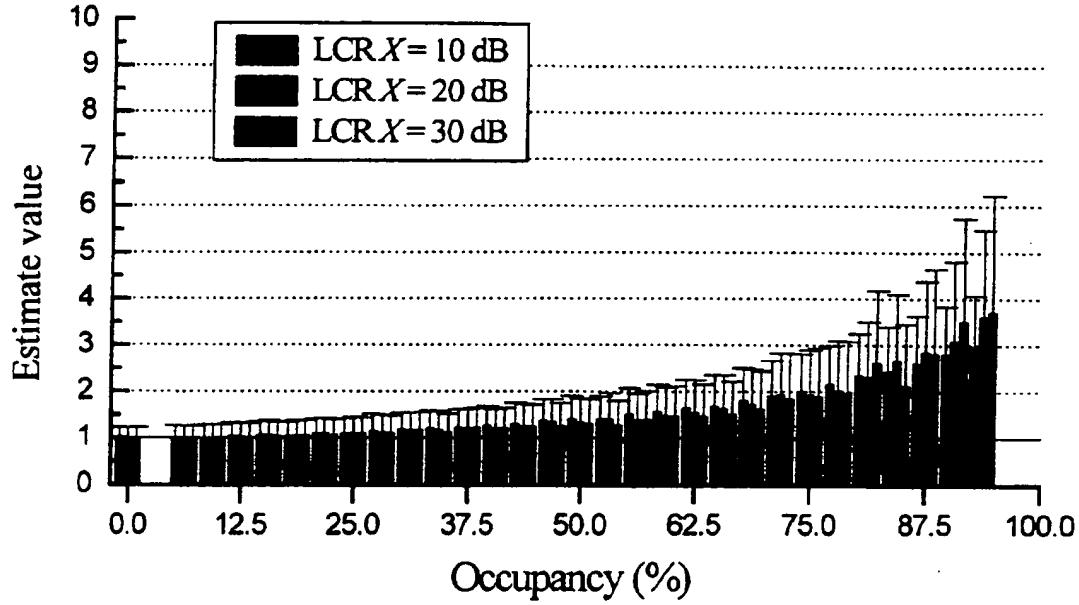

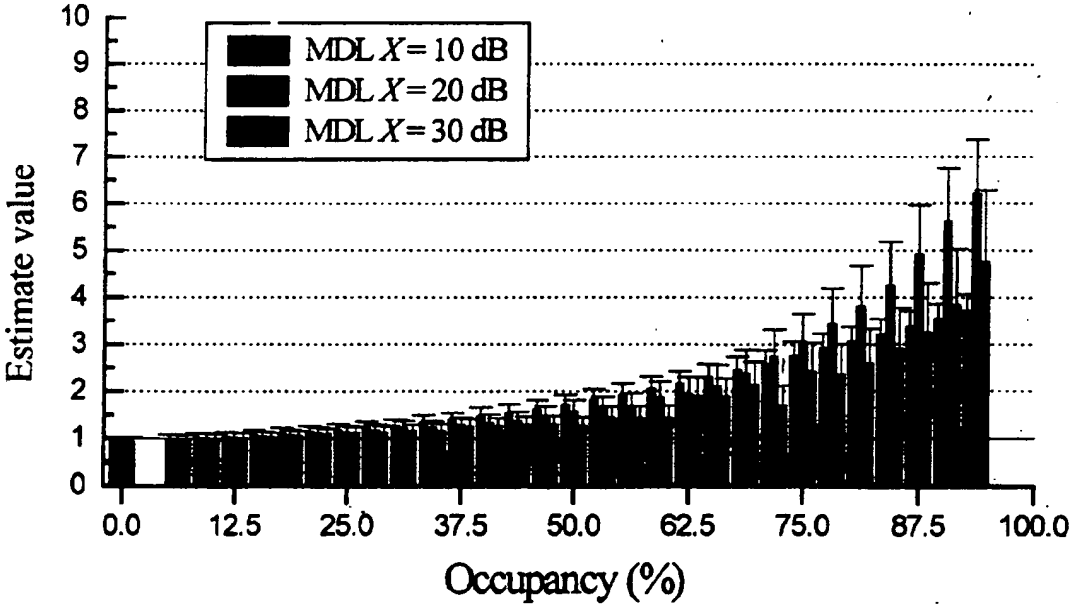

Figure 6. Noise floor level estimation for dBr power, $K = 8$, $M = 64$, and BFSK signal.

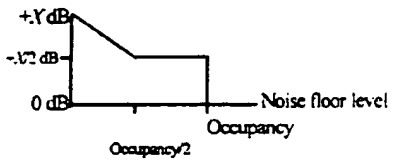

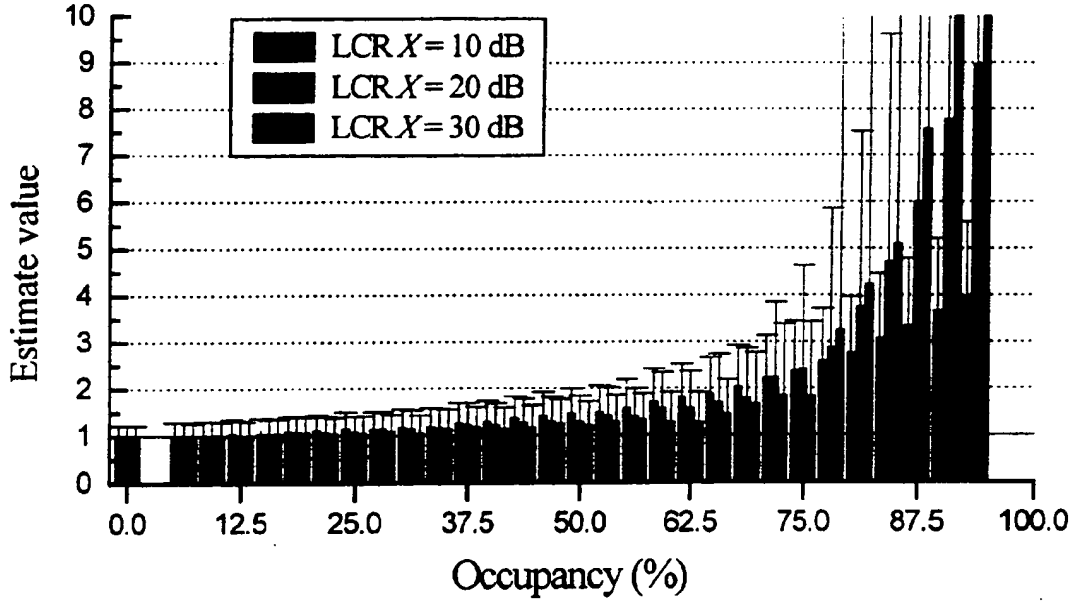

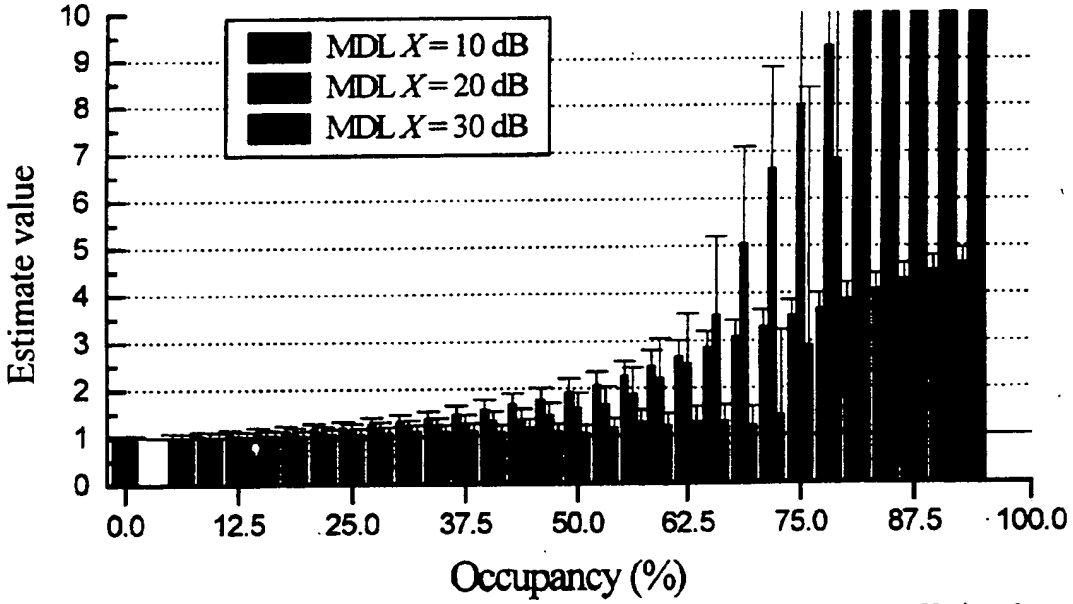

Figure 7. Noise floor level estimation for dBre power, $K = 8$, $M = 64$, and BFSK signal.

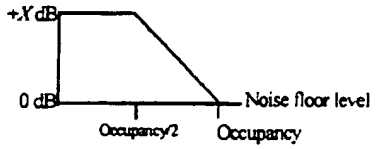

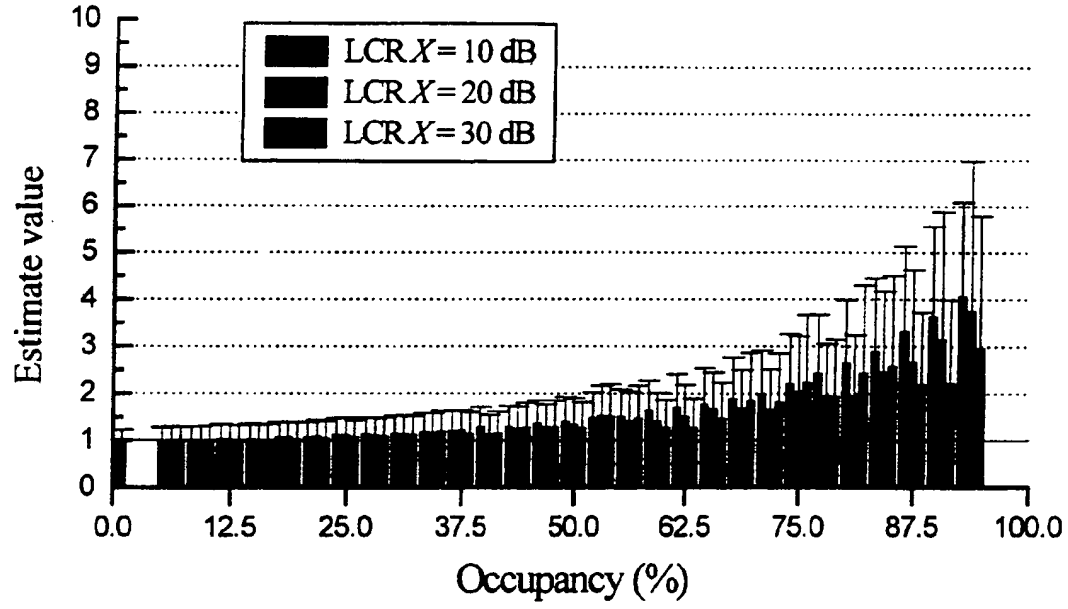

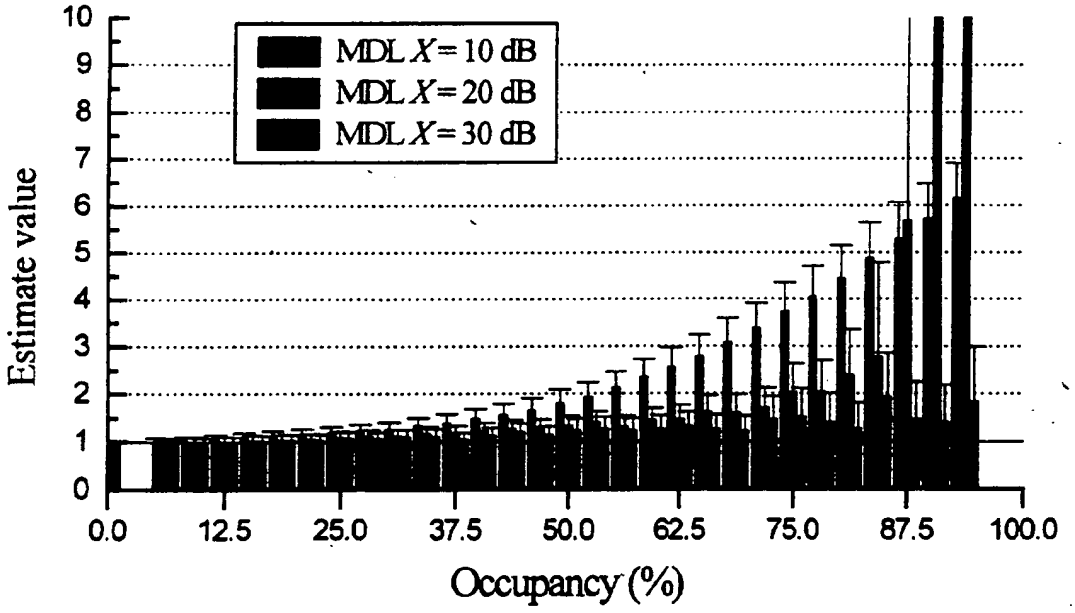

Figure 8. Noise floor level estimation for dBer power, $K = 8$, $M = 64$, and BFSK signal.

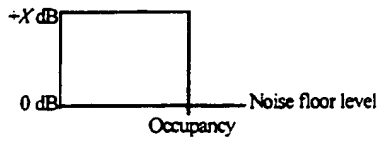

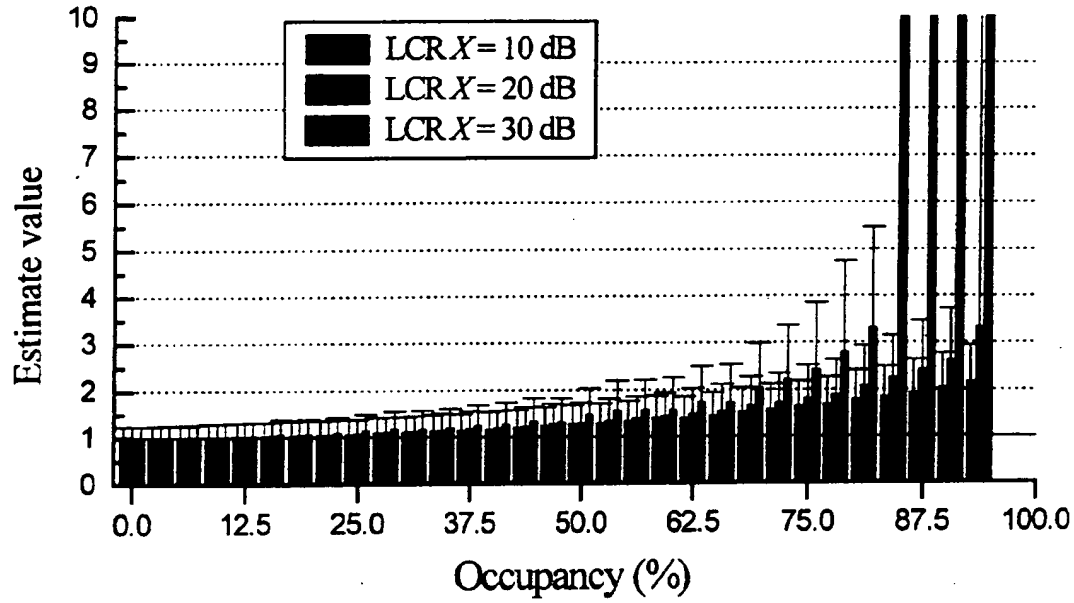

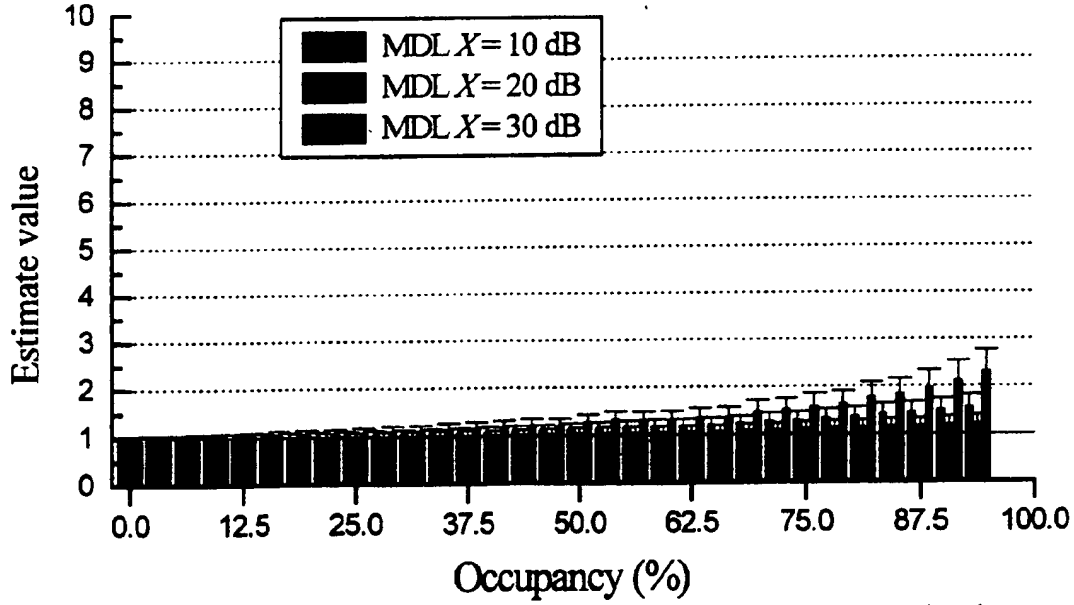

Figure 9. Noise floor level estimation for dBe power, $K = 8$, $M = 64$, and FM signal.

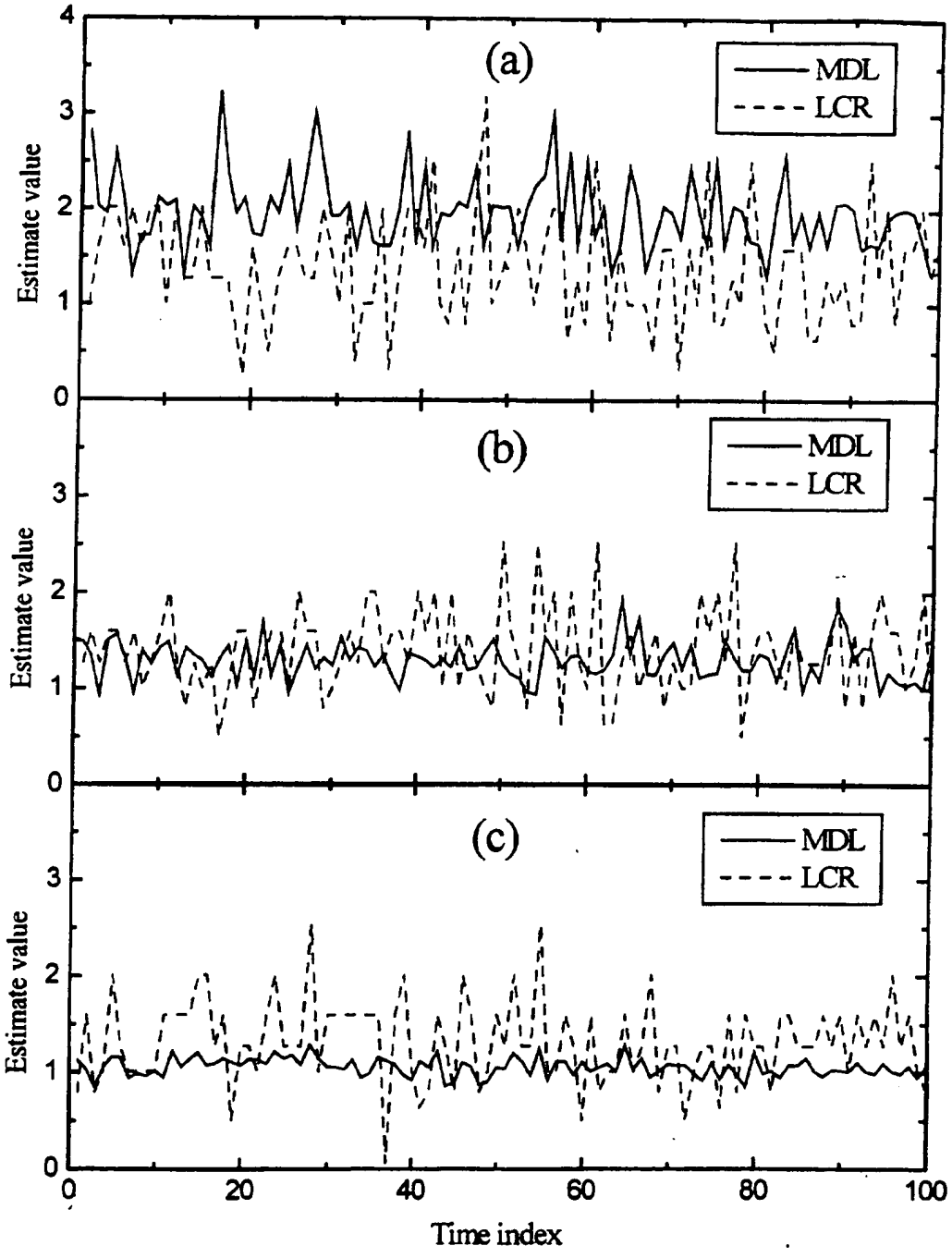

Figure 10. Noise floor estimate variations at 50 % occupancy with $K = 8$ and $M = 64$.
(a) BFSK signal at 10 dB SNR with equal power levels,
(b) BFSK signal at 20 dB SNR with equal-ramp power levels,

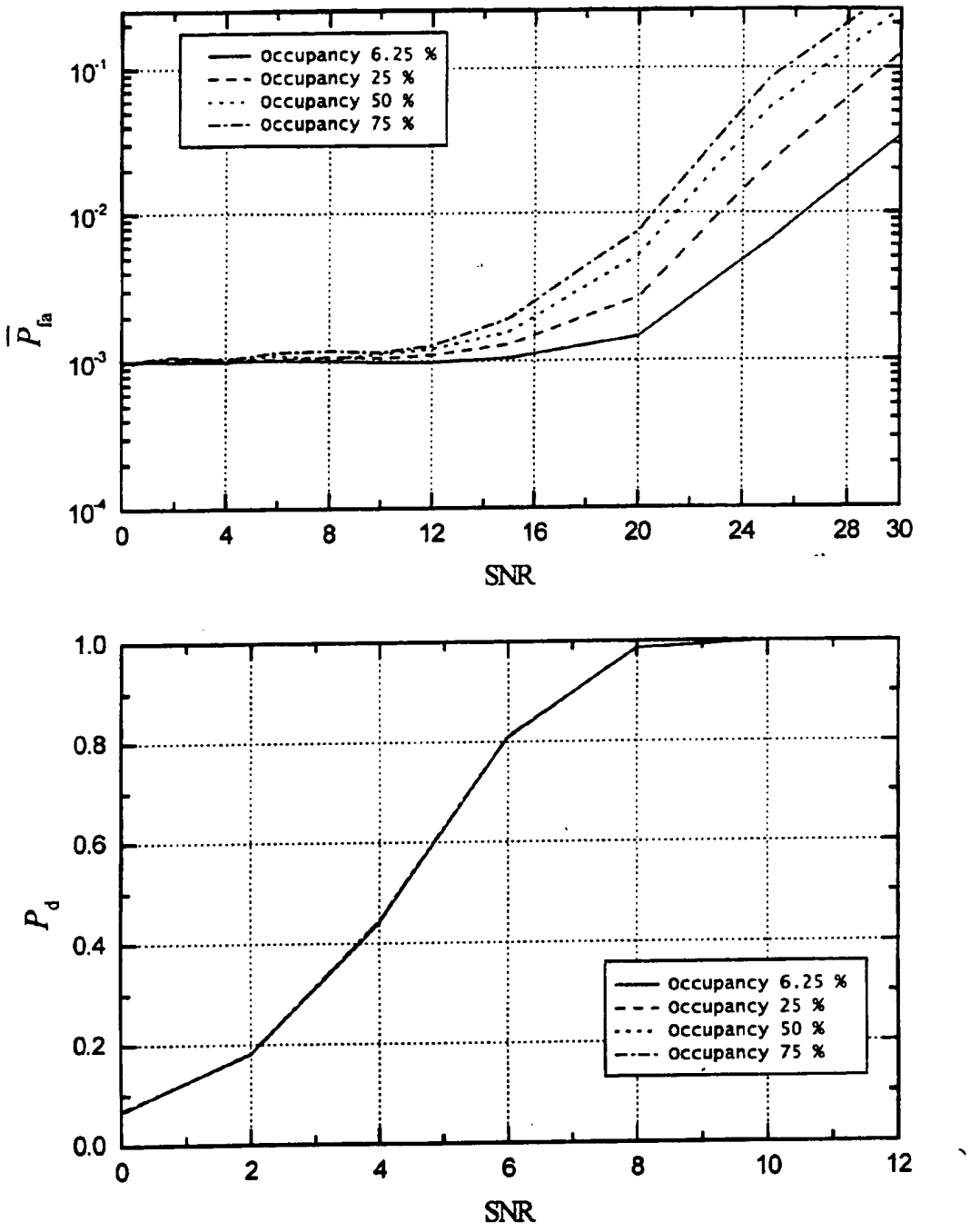

Figure 11. $\overline{P}_{fa}$ and P_d for the BFSK signal with equal-ramp power, 64 channels, 6 bins of out 8 for detection, and known SNR.

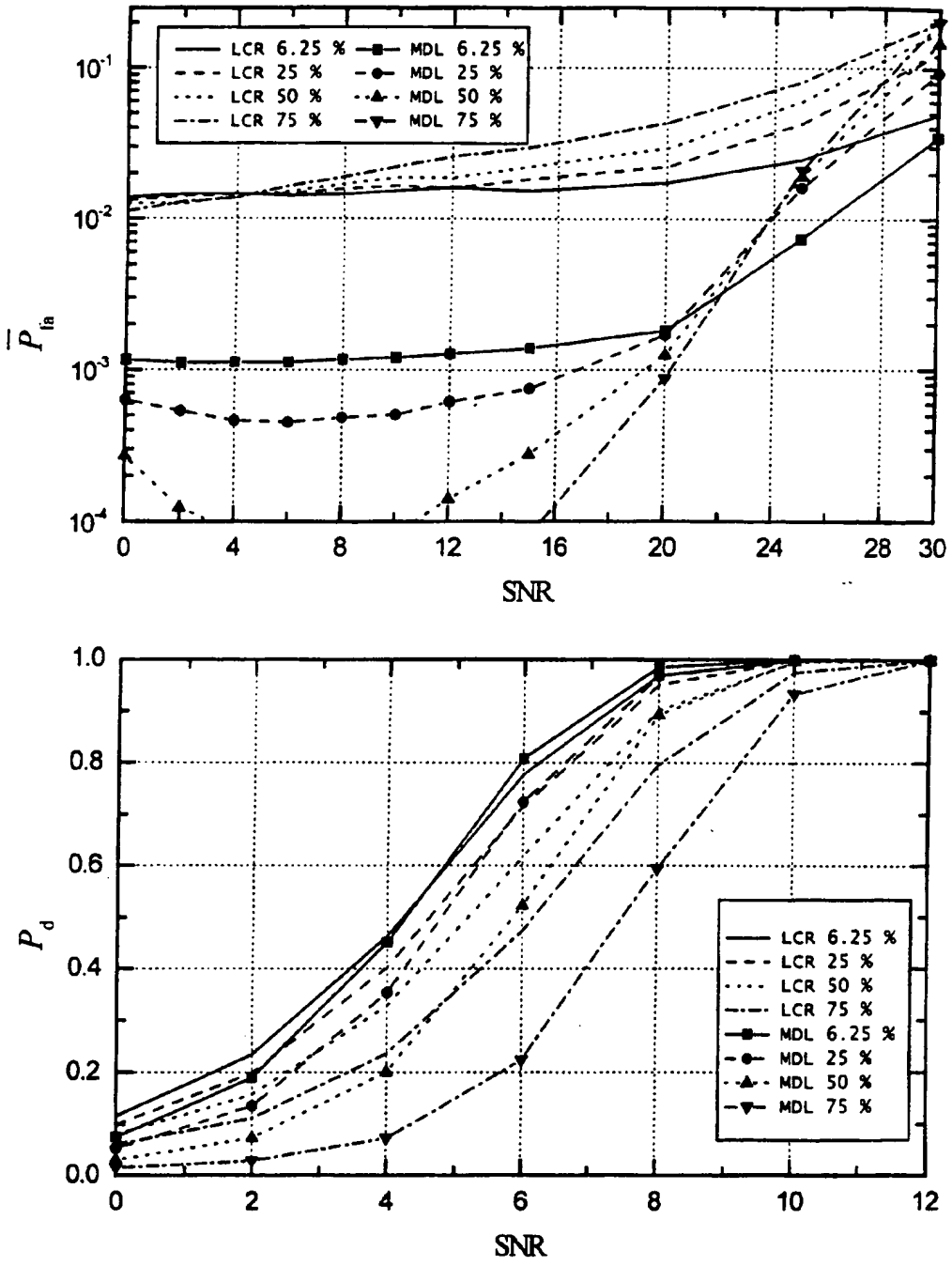

Figure 12. $\overline{P}_{fa}$ and P_d for the BFSK signal with equal-ramp power, 64 channels, 6 bins of out 8 for detection, and 1 average of the noise floor estimate.

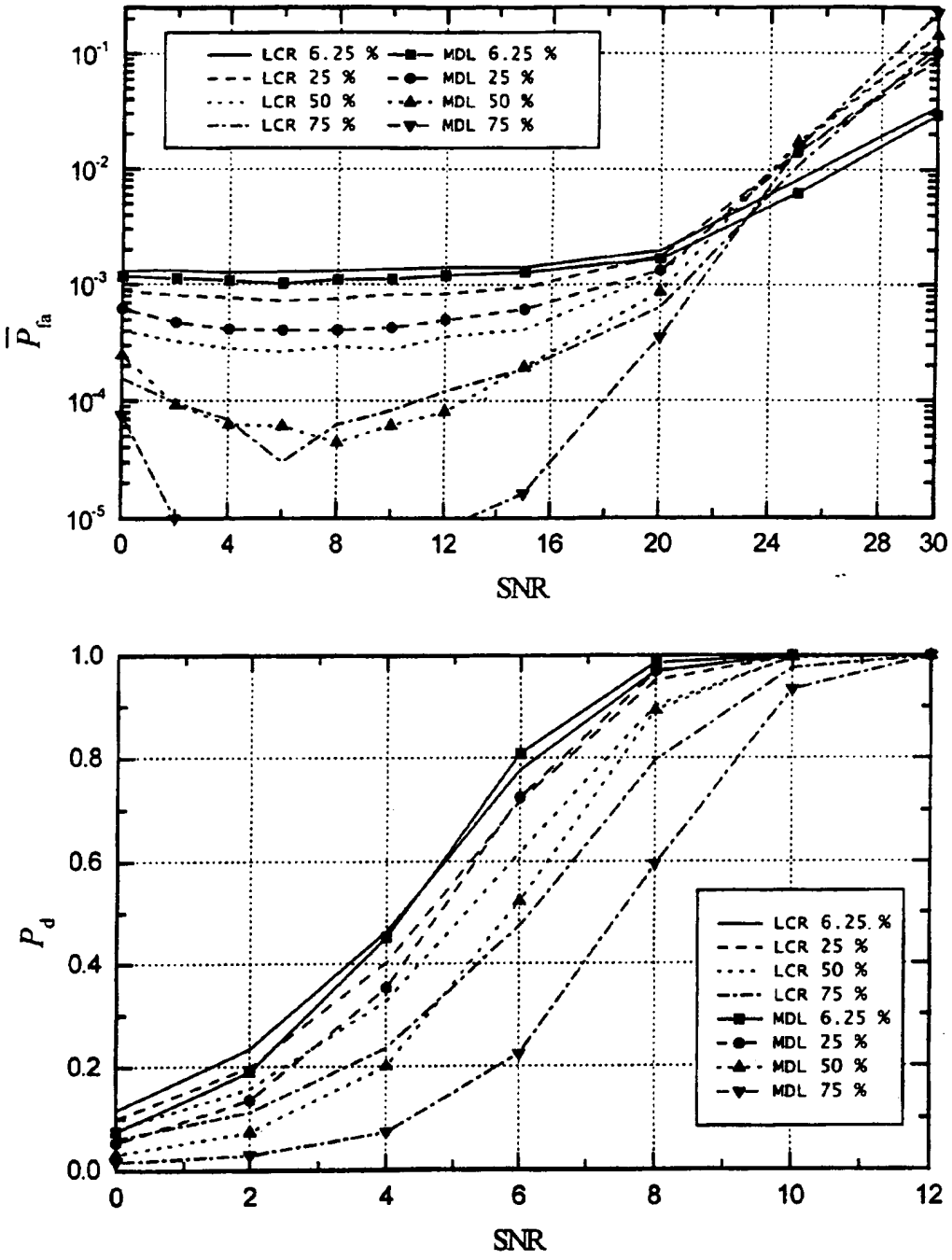

Figure 13. $\overline{P}_{fa}$ and P_d for the BFSK signal with equal-ramp power, 64 channels, 6 bins of out 8 for detection, and 10 averages of the noise floor estimate.

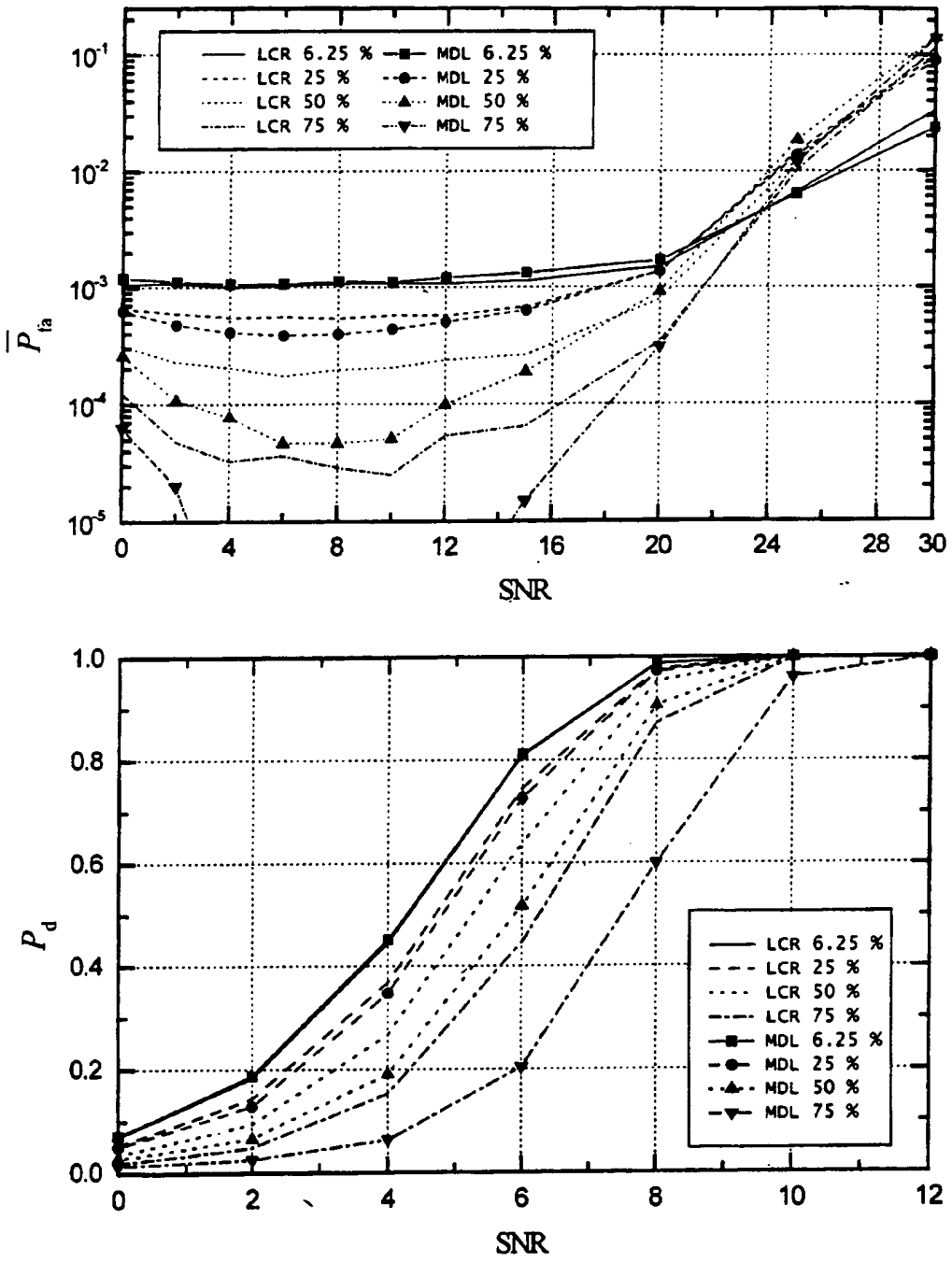

Figure 14. $\overline{P}_{fa}$ and P_d for the BFSK signal with equal-ramp power, 64 channels, 6 bins of out 8 for detection, and 100 averages of the noise floor estimate.

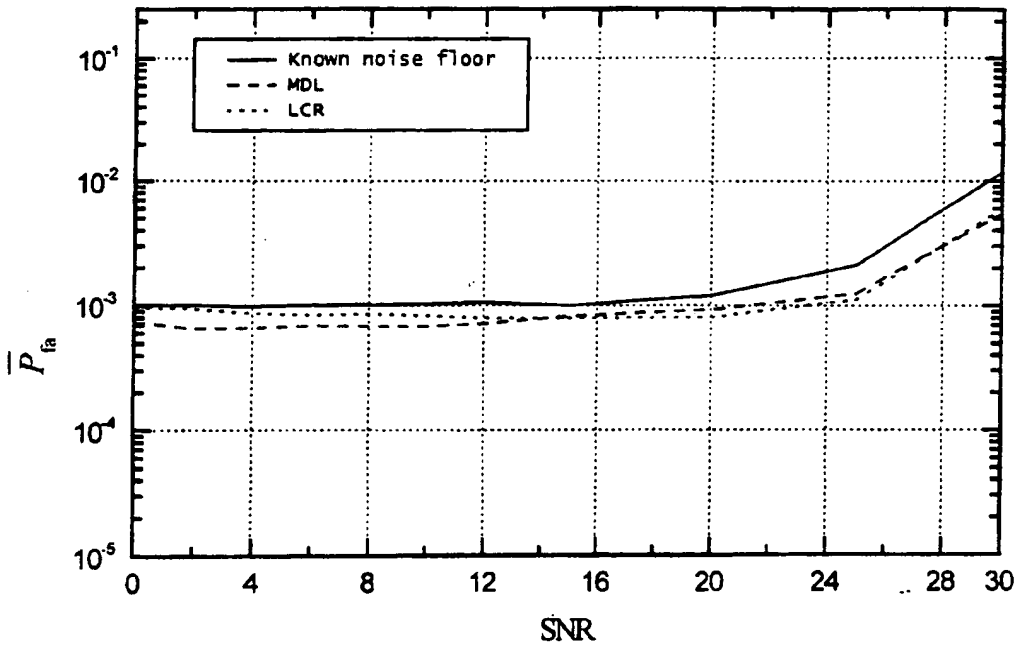

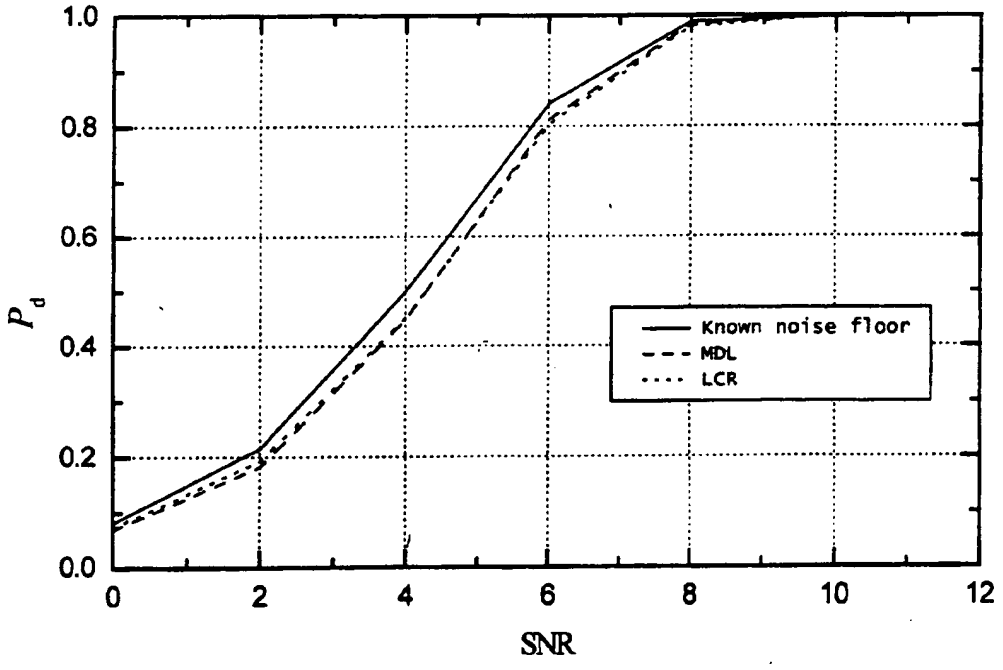

Figure 15. $\overline{P}_{fa}$ and P_d for the FM signal with equal-ramp power, 25 % occupancy, 64 channels, 6 bins of out 8 for detection, and 10 averages of the noise floor estimate.

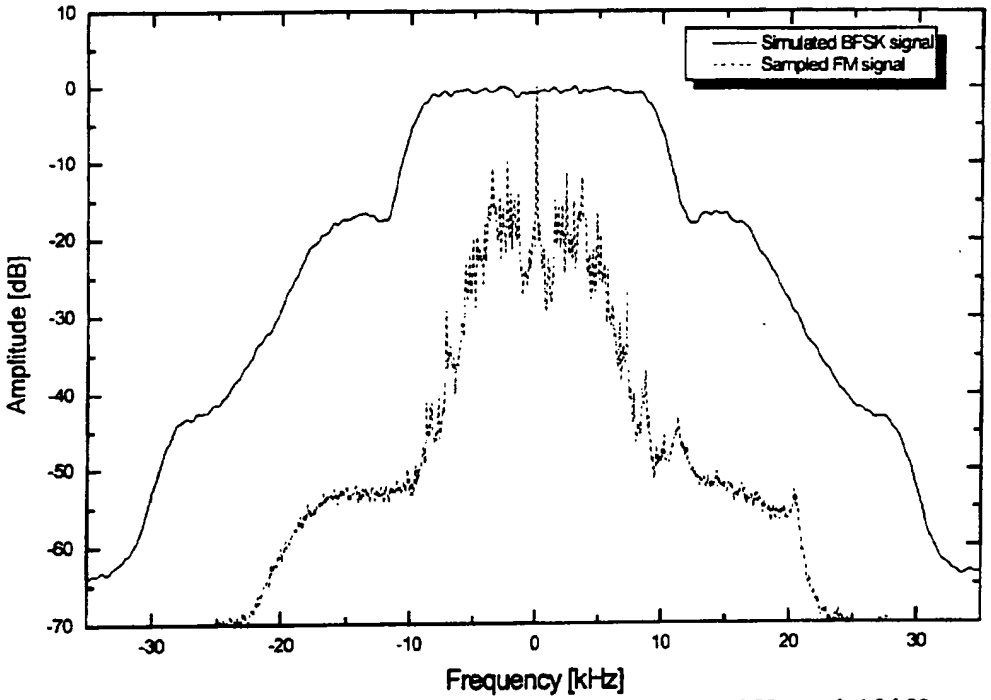

Figure 16. Average spectrum of BFSK and FM signals with 25 kHz and 15 kHz nominal channel bandwidth respectively

References

[Aus95] M.D. Austin, and G.L. Stüber, "In-Service Signal Quality Estimation for TDMA Cellular Systems," *Proceedings of the 6th IEEE International Symposium on Personal, Indoor and Mobile Radio Communications*, vol. 2, pp.836-840, 1995.

[Kel86] E.J. Kelly, "An Adaptive Detection Algorithm," *IEEE Trans. on Aero. and Electro. Syst.*, vol. 22, no. 1, pp. 115-127, 1986.

[Lee69] W.C.Y. Lee, "Finding the Statistical Properties of the Median Values of a Fading Signal Directly from Its Decibel Values," *Proceedings of the IEEE*, vol. 58, pp. 278-288, Feb. 1970.

[Lee82] W.C.Y. Lee, Mobile Communications Engineering, McGraw-Hill, 1982.

[Loo98] C. Loo, and J.S. Butterworth, "Land Mobile Satellite Channel Measurements and Modelling," *Proc. of the IEEE*, vol. 86, no. 7, pp. 1442-1463. July 1998.

[Max85] M. Wax, and T. Kailath, "Detection of Signals by Information Theoretic Criteria," *IEEE Trans. Acoust., Speech, Signal Processing*, vol. 33, no. 2, pp. 387-392, April 1985.

[Pat97] F. Patenaude, and D. Boudreau, "CFAR Detection Based on FFT and Polyphase FFT Filter Banks: Known SNR," *CRC Technical Memorandum*, VPCS # 22/97, December 1997.

[Pau95] D.R. Pauluzzi, and N.C. Beaulieu, "A Comparison of SNR Estimation Techniques in the AWGN Channel," *Proceedings of IEEE Pacific Rim Conference on Communications, Computers, and Signal Processing*, pp. 36-39, 1995.

[Rea97] M.J. Ready, M.L. Downey, and L.J. Corbalis, "Automatic Noise Floor Spectrum Estimation in the Presence of Signals," *Proceedings of the 31rd Asilomar Conference on Signals, Systems and Computers*, vol. 1, pp. 877-881, Nov. 1997.

[Ric48] S.O. Rice, "Statistical Properties of a Sine Wave Plus Random Noise," *Bell System Technical Journal*, vol. 27 pp. 109-157, Jan. 1948.

[Sto92] P. Stoica, T. Söderström, and V. Šimonytė, "On Estimating the Noise Power in Array Processing," *Signal Processing*, vol. 26, no. 2, pp.205-220, Feb. 92.

CLAIMS

1. A method for recognizing the type of modulation of a signal, comprising the steps of

examining the signal for amplitude variations for identifying the signal as one of an envelope and non-constant envelope signal;

estimating the carrier frequency and correcting for carrier frequency errors; and

categorizing the modulation of the signal.

2. The method of claim 1, wherein when the signal is identified as a constant envelope signal, the step of estimating the carrier frequency comprises the steps of

processing the signal by a Fast Fourier Transform (FFT) of the input signal;

obtaining the square of the absolute value obtained; and

searching for the maximum frequency sample.

3. The method of claim 2, wherein the FFT is with zero paddng.

4. The method of claim 2, wherein the step of searching comprises a coarse search and a fine search.

5. The method of claim 1, wherein when the signal is identified as a non-constant envelope signal, the step of estimating the carrier frequency comprises the steps of

in a first path, processing the signal by a Fast Fourier Transform (FFT) to produce a first output;

in a second path, passing the signal through a square law non-linearity before processing by a FFT to produce a second output;

in a third path, passing the signal through a fourth law non-linearity before processing by a FFT to produce a third output; and

selecting a maximum energy sample among the first, second and third outputs as a normalized frequency estimate;

whereby the first path is selected when the signal is an AM signal, the second path is selected when the signal is a DSB-SC or BPSK signal, and the third path is selected when the signal is a QPSK signal.

6. The method of claim 2, including the further step of dividing the signal into Continuous Wave (CW) and Frequency Modulated (FM) signals by obtaining a value of the variance of the unwrapped phase (direct phase) for signal samples above a preselected threshold; and classifying the signal as a CW signal when the variance is substantially zero and as a FM signal when the variance is significantly above zero.

7. The method of claim 6, wherein the threshold is equal to a mean of an amplitude of the signal.

8. The method of claim 7, wherein a FM signal is identified as one of a digital and analog frequency modulated signal by determining the kurtosis coefficient of the instantaneous frequency distribution of the signal, the kurtosis coefficient being the fourth normalized moment, centered about the mean, of the instantaneous frequency of the signal, and

classifying the signal as an analog frequency modulated signal when the coefficient is at least 2.5 and as a digital frequency modulated signal when the coefficient is below 2.5.

9. The method of claim 8, wherein the instantaneous frequency is obtained by computing the phase derivative of the signal and the method comprises the additional step of, prior to computing the instantaneous frequency, filtering the phase signal.

10. The method of claim 9, wherein the step of filtering comprises

estimating an effective bandwidth of the phase signal; and

filtering the phase signal with a low-pass filter having a cut-off frequency above the bandwidth.

11. A method for estimating the noise floor of a signal, comprising the steps of

determining a FFT trace output from the signal;

quantifying the value of the output to the nearest integer dB value;

creating an empty histogram with bins from a minimum value to a maximum value;

for every positive slope segment of the histogram curve adding 1 to the histogram bin which is crossed by the curve, except the end point of the curve segment;

finding a first local maximum of the curve, starting from the lowest dB values;

checking if another local maximum is present XdB higher than the current maximum;

setting the current maximum as the noise floor position if no other local maximum is present XdB higher than the current maximum;

repeating the step of checking until no other local maximum is present;

finding the noise floor per channel by applying a dB correction of dB value of noise floor per bin + 10 log10 (number of bins used per channel) + 3.

12. A method for estimating the noise floor of a signal, comprising the steps of

building a histogram from a FFT output trace quantified to the nearest integer dB value;

transferring the histogram into a sorter linear vector;

channeling the sorted linear vector into M groups;

adding the penalty polynomial function to the negative of the log-likelihood;

finding an index of the global minimum;

estimating the noise floor as the average of the last M minus the index number smallest sorted groups.